Cellular/Molecular

Cerebellar Ataxia by Enhanced $Ca_V2.1$ Currents Is Alleviated by Ca^{2+}-Dependent K^+-Channel Activators in *Cacna1a*^{S218L} Mutant Mice

Zhenyu Gao,[1] Boyan Todorov,[2] Curtis F. Barrett,[2,3] Stijn van Dorp,[4] Michel D. Ferrari,[3] Arn M.J.M. van den Maagdenberg,[2,3] Chris I. De Zeeuw,[1,4] and Freek E. Hoebeek[1]

[1]Department of Neuroscience, Erasmus Medical Centre, 3000 CA Rotterdam, Netherlands; [2]Department of Human Genetics, and [3]Department of Neurology, Leiden University Medical Centre, 2300 RC Leiden, Netherlands; [4]Netherlands Institute for Neuroscience, Royal Academy of Arts & Sciences (KNAW), 1105 BA Amsterdam, Netherlands

Mutations in the *CACNA1A* gene are associated with neurological disorders, such as ataxia, hemiplegic migraine, and epilepsy. These mutations affect the pore-forming α_{1A}-subunit of $Ca_V2.1$ channels and thereby either decrease or increase neuronal Ca^{2+} influx. A decreased $Ca_V2.1$-mediated Ca^{2+} influx has been shown to reduce the regularity of cerebellar Purkinje cell activity and to induce episodic cerebellar ataxia. However, little is known about how ataxia can be caused by *CACNA1A* mutations that increase the Ca^{2+} influx, such as the S218L missense mutation. Here, we demonstrate that the S218L mutation causes a negative shift of voltage dependence of $Ca_V2.1$ channels of mouse Purkinje cells and results in lowered thresholds for somatic action potentials and dendritic Ca^{2+} spikes and in disrupted firing patterns. The hyperexcitability of *Cacna1a*^{S218L} Purkinje cells was counteracted by application of the activators of Ca^{2+}-dependent K^+ channels, 1-EBIO and chlorzoxazone (CHZ). Moreover, 1-EBIO also alleviated the irregularity of Purkinje cell firing both *in vitro* and *in vivo*, while CHZ improved the irregularity of Purkinje cell firing *in vitro* as well as the motor performance of *Cacna1a*^{S218L} mutant mice. The current data suggest that abnormalities in Purkinje cell firing contributes to cerebellar ataxia induced by the S218L mutation and they advocate a general therapeutic approach in that targeting Ca^{2+}-dependent K^+ channels may be beneficial for treating ataxia not only in patients suffering from a decreased Ca^{2+} influx, but also in those suffering from an increased Ca^{2+} influx in their Purkinje cells.

Introduction

The entry of Ca^{2+} ions via voltage-gated Ca^{2+} channels (VGCCs) controls crucial processes in mammalian neurons, such as neurotransmitter release, synaptic plasticity, and membrane excitability. Mutations that affect VGCC functioning have severe clinical consequences (Catterall et al., 2008). For instance, various mutations in the *CACNA1A* gene, which codes for the α_{1A}-subunit of $Ca_V2.1$ (P/Q-type) VGCCs, are associated with various clinical neurological disorders including ataxia, hemiplegic migraine, and epilepsy (Ophoff et al., 1996; Jouvenceau et al., 2001).

An increase or decrease in $Ca_V2.1$-mediated Ca^{2+} influx results in different clinical manifestations: *CACNA1A* gene mutations that increase $Ca_V2.1$-mediated Ca^{2+} influx are linked to familial hemiplegic migraine type 1 (FHM1) (Pietrobon, 2007), whereas episodic ataxia type 2 is linked to mutations in the *CACNA1A* gene that decrease $Ca_V2.1$-mediated Ca^{2+} influx (Ophoff et al., 1996; van den Maagdenberg et al., 2007). Studies of ataxic mouse models, such as *tottering* and *leaner* mice (Fletcher et al., 1996; Mori et al., 2000) that carry mutations in the orthologous mouse *Cacna1a* gene revealed that a decreased $Ca_V2.1$-mediated Ca^{2+} influx consistently results in disrupted Purkinje cell firing activity (Hoebeek et al., 2005; Walter et al., 2006).

Although the link between a reduction in $Ca_V2.1$-mediated Ca^{2+} influx and ataxia has been explored using mutant mouse models (Pietrobon, 2010), it remains to be elucidated why ataxia can also occur in FHM1 patients who suffer from an enhanced $Ca_V2.1$-mediated Ca^{2+} influx (Kors et al., 2001; Tottene et al., 2005). For instance, patients with the serine to leucine missense mutation at position 218 (S218L) of the α_{1A}-subunit, which enhances the $Ca_V2.1$-mediated Ca^{2+} influx, are also severely ataxic (Kors et al., 2001; Tottene et al., 2005). Here we performed detailed electrophysiological analyses of Purkinje cell excitability

Received May 20, 2012; revised Aug. 28, 2012; accepted Sept. 4, 2012.

Author contributions: Z.G., B.T., C.F.B., S.v.D., M.D.F., A.M.J.M.v.d.M., C.I.D.Z., and F.E.H. designed research; Z.G. and F.E.H. performed research; Z.G. and F.E.H. analyzed data; Z.G., B.T., C.F.B., A.M.J.M.v.d.M., C.I.D.Z., and F.E.H. wrote the paper.

Support for this work was provided from The Netherlands Organization for Scientific Research (NWO) NWO-ALW and NWO-ZON-MW (C.I.D.Z. and F.E.H.), NeuroBasic-PharmaPhenomics, EEC-SENSOPAC, and Prinses Beatrix Fonds (C.I.D.Z.), Erasmus University Rotterdam fellowship (F.E.H.), Vici 918.56.602 (M.D.F.), and the Center of Medical System Biology established by the Netherlands Genomics Initiative/Netherlands Organisation for Scientific Research and Community (M.D.F. and A.M.J.M.v.d.M.). Funders had no role in study design, data collection and analysis, decision to publish, or preparation of the manuscript. We are grateful to E. Haasdijk, E. Goedknegt, M. Rutteman, P. Plak, and Dr. E. Dalm for technical assistance; to Dr. J.G.G. Borst, Dr. Hitoshi Morikawa, E. Galliano, and B. van Beugen for constructive discussions; and to Dr. I. Raman for advice on dissociated Purkinje cell preparation.

This article is freely available online through the *J Neurosci* Open Choice option.

The authors declare no competing financial interests.

Correspondence should be addressed to Chris I. De Zeeuw, Department of Neuroscience, Erasmus Medical Center, Dr. Molewaterplein 40, 3015 GD Rotterdam, Netherlands. E-mail: c.dezeeuw@erasmusmc.nl.

C.F. Barrett's present address: English Editing Solutions, Oegstgeest 2343KW, The Netherlands.

DOI:10.1523/JNEUROSCI.2454-12.2012

 0270-6474/12/3215533-14$15.00/0

and their activity patterns in *Cacna1a*^{S218L} knock-in mice in which the FHM1 S218L mutation was introduced in the *Cacna1a* gene (van den Maagdenberg et al., 2010). Our results show that the Purkinje cells in these mutants have distinct irregular activity patterns, both *in vitro* and *in vivo*. Both the irregular Purkinje cell spiking and ataxic motor performance can be counteracted by activators of small-conductance Ca^{2+}-activated K^+ channels (SK channels), but not by SK-channel inhibitors. Our data suggest a novel mechanism that underlies ataxia in *Cacna1a* mutants characterized by an increased $Ca_V2.1$-mediated Ca^{2+} influx. Together with the data obtained in *Cacna1a* mutants with a reduced $Ca_V2.1$-mediated Ca^{2+} influx, our results demonstrate a narrow window in Ca^{2+} homeostasis: both sufficiently decreased and increased Ca^{2+} influx can induce ataxia.

Materials and Methods

Animals. *Cacna1a*^{S218L} mice were generated as previously described (van den Maagdenberg et al., 2010). Heterozygous male and female offspring (generated by C57BL/6J × heterozygous *Cacna1a*^{S218L} breeding) were crossed to generate homozygous *Cacna1a*^{S218L} mice and wild-type (WT) littermates. Offspring of both genders ranging from postnatal day 16 (P16) to 3 months old were used in the experiments. Animals were housed at 22 ± 2°C in a 12 h dark/light cycle and were provided with food and water *ad libitum*. All studies were performed with experimenters blind to the genotype and in accordance with the guidelines of the respective universities and national legislation.

Slice preparation for electrophysiology. *Cacna1a*^{S218L} mutants and WT littermates were decapitated under isoflurane anesthesia. Subsequently, the cerebellum was removed and transferred into ice-cold slicing medium that contains the following (in mM): 240 sucrose, 5 KCl, 1.25 Na_2HPO_4, 2 $MgSO_4$, 1 $CaCl_2$, 26 $NaHCO_3$, and 10 D–glucose, bubbled with 95% O_2 and 5% CO_2. Parasagittal slices (200 or 250 μm thick) of the cerebellar vermis were cut using a Leica vibratome (VT1000S) and kept in artificial CSF (ACSF) containing the following (in mM): 124 NaCl, 5 KCl, 1.25 Na_2HPO_4, 2 $MgSO_4$, 2 $CaCl_2$, 26 $NaHCO_3$, and 20 D–glucose, bubbled with 95% O_2 and 5% CO_2 for >1 h at 34°C before the experiments started. All drugs were purchased from Tocris Bioscience unless stated otherwise.

Whole-cell electrophysiology. Experiments were performed with a constant flow of oxygenated ACSF (1.5–2.0 ml/min). Purkinje cells were visualized using an upright microscope (Axioskop 2 FS plus; Carl Zeiss) equipped with a 40× water-immersion objective. Patch-clamp recordings were performed using an EPC-10 double amplifier (HEKA Electronics). Voltage-clamp recordings were performed at room temperature, whereas current-clamp and loose cell-attached recordings were performed at 34 ± 1°C. *In vitro* experiments were performed in the presence of picrotoxin (PTX; 100 μM), 1,2,3,4-tetrahydro-6-nitro-2,3-dioxo-benzo-(*f*)-quinoxaline-7-sulfonamide disodium salt hydrate (NBQX; 10 μM) and D-(−)-2-amino-5-phosphonopentanoic acid (D-AP5; 10 μM) unless stated otherwise.

Ca^{2+} current and Ca^{2+}-dependent K^+ current in dissociated Purkinje cells. Purkinje cells were isolated enzymatically from P16 to P21 WT and *Cacna1a*^{S218L} cerebellum using a protocol adapted from Raman and Bean (1999). Coronal slices of 250 or 300 μm thick were incubated in dissociation solution containing the following (in mM): 69 Na_2SO_4, 30 K_2SO_4, 5 $MgCl_2$, 25 $NaHCO_3$, and 10 D–glucose, supplemented with 3 mg/ml protease XXIII and oxygenated with 95% O_2 and 5% CO_2 at 32°C for 7 min. After incubation, slices were washed three times with warm dissociation solution containing 1 mg/ml trypsin inhibitor and 1 mg/ml bovine serum albumin, and subsequently washed in Tyrode's solution containing the following (in mM): 150 NaCl, 4 KCl, 2 $CaCl_2$, 2 $MgCl_2$, 10 HEPES, and 10 D–glucose at room temperature. Slices were triturated in Tyrode's solution with fire-polished Pasteur pipettes to liberate individual neurons. Neurons were suspended and mounted on poly-D-lysine/Laminin-coated coverslips (BD Biosciences) for further experiments. Purkinje cells were identified by their large diameter and pear-shaped soma. To ensure an adequate voltage-clamp, only Purkinje cells that lost most of the primary dendrites were selected. Whole-cell Ca^{2+} currents were recorded in dissociated Purkinje cells from *Cacna1a*^{S218L} and WT animals using an intracellular solution containing the following (in mM): 100 $CsMeSO_4$, 2 $MgCl_2$, 20 tetraethylammonium (TEA), 10 EGTA, 5 QX-314, 10 HEPES, 10 Na-Phosphocreatine, 4 Na_2ATP, and 0.4 Na_3GTP, pH 7.3. In addition, 1 μM tetrodotoxin (TTX) and 2.5 mM 4-aminopyridin (4-AP) were added to the ACSF to block voltage-gated Na^+ and K^+ currents, respectively. The series resistance was compensated for >70% and leak and capacitive currents were subtracted by the P/4 method. Cells were discarded when the holding current at −70 mV exceeded −100 pA. The reported membrane potentials were corrected off-line for the junction potential (the real membrane potential was 10.2 mV more hyperpolarized than measured).

Ca^{2+} currents were obtained by 50 ms depolarizing pulses to various membrane potentials ranging between −70 and +40 mV at 5 mV increments. Current–voltage (I-V) curves were obtained only from cells with a voltage error of <5 mV and without any sign of inadequate voltage-clamp as identified by notch-like current discontinuities and slow components in the decay of capacitance currents (in response to hyperpolarizing pulses). The current density was calculated by dividing the current amplitude by the cell's capacitance. We consider currents > 3 SD from the average holding current detectable. The conductance was calculated for each cell from the current–voltage relations using the following formula: $G = I/(V_m - V_r)$, I is the current density measured with each depolarizing pulse, V_m is the corresponding depolarizing voltage, and V_r is the reversal potential. $Ca_V2.1$ blocker ω-Agatoxin-IVA (Peptide Institute, Osaka, Japan) was prepared in ACSF in the presence of 1 mg/ml cytochrome *c* to minimize nonspecific binding. Stock solutions (0.1 mM concentrations) were stored at −20°C and used within 2 weeks. The stock solutions were diluted in ACSF supplemented with 0.1 mg/ml cytochrome *c*, yielding a final ω-Agatoxin-IVA concentration of 0.2 μM. To estimate the Ca^{2+}-dependent K^+ channels, whole-cell currents were measured with intracellular solution containing the following (in mM): 120 K-Gluconate, 9 KCl, 10 KOH, 3.48 $MgCl_2$, 4 NaCl, 10 HEPES, 4 Na_2ATP, 0.4 Na_3GTP, and 17.5 sucrose, pH 7.25. One micromolar of TTX, 2.5 mM 4-AP and 1 mM TEA were added to ACSF to block voltage-gated Na^+-channels and most of voltage-gated K^+-dependent and large-conductance Ca^{2+}-dependent K^+ channels (Raman and Bean, 1999; Cingolani et al., 2002). To estimate the remaining Ca^{2+}-dependent K^+ channels, we adopted a protocol used previously to isolate SK-mediated tail currents in Purkinje cells (Cingolani et al., 2002). The Ca^{2+} influx was obtained by 50 ms depolarizing pulses to various membrane potentials ranging between −70 mV and +20 mV. A positive tail current after the depolarizing pulse was measured as an indication of Ca^{2+}-dependent K^+ channels. To estimate the ratio between Ca_V and SK conductances in Purkinje cells, Ca^{2+}-dependent K^+ currents were first measured in Tyrode's solution supplemented with 2.5 mM 4-AP, 1 mM TEA, and 1 μM TTX, pH 7.25. After a stable I-V curve was obtained, the extracellular solution was replaced by the second extracellular solution containing the following (in mM): 165 TEA-Cl, 2 $BaCl_2$, 10 HEPES, 2.5 4-AP, and 0.001 TTX, pH 7.25, to isolate the Ba^{2+} current. I-V curves were constructed from data obtained after a stable Ba^{2+} current was achieved. SK- and Ba^{2+}-current densities of <5 pA/pF were excluded to avoid inaccurate analysis of the ratio between these currents for each Purkinje cell.

Purkinje cell spontaneous activity and current-clamp recording. The Purkinje cell spiking activity was recorded in loose cell-attached configuration with patch pipettes (diameter 2–3 μm) filled with ACSF at 34 ± 1°C. Two- to three-month-old *Cacna1a*^{S218L} mutants and WT littermates were used in this experiment. Spontaneous activity was observed as fast current deflections of −100 to −200 pA. Analysis of the regularity of spiking and the frequency was performed with MATLAB (MathWorks) and Excel (Microsoft) using the first 5000 spikes recorded from each cell. The instantaneous regularity of firing was calculated using the coefficient of variance (CV) of interspike-intervals (ISIs) (CV = stdev (ISI)/mean (ISI)) and the CV2 of ISIs: $(CV2 = 2|ISI_{n+1} - ISI_n|/(ISI_{n+1} + ISI_n))$ (Holt et al., 1996). Bursts of action potentials were defined as a train of at least three spikes with an instantaneous firing frequency of >3× the average firing frequency, followed by a pause of >100 ms.

Current-clamp experiments were performed at 34 ± 1°C using an intracellular solution containing the following (in mM): 120 K-Gluconate, 9 KCl, 10 KOH, 3.48 $MgCl_2$, 4 NaCl, 10 HEPES, 4 Na_2ATP, 0.4 Na_3GTP, and 17.5 sucrose, pH 7.25. The membrane potential of Purkinje cells from 2- to 3-month old *Cacna1a*^{S218L} and WT animals was held at −65 to −70 mV using −400 to −500 pA current injection to avoid spontaneous spiking activity. To study the effects of parallel fiber (PF) input on Purkinje cell spiking patterns we canceled all current injections to allow spontaneous firing. We recorded the intrinsic excitability by injecting depolarizing currents ranging from 100 to 1000 pA relative to the holding current. The junction potential (calculated to be 9 mV) was not corrected for current-clamp experiments.

Simultaneous recordings from a Purkinje cell soma and dendrite were performed in a separate set of experiments using P21–P30 animals. Both somatic and dendritic recordings were obtained in current-clamp. Dendritic spikes and back-propagated action potentials were readily identified by amplitude, rise time, and decay time constant (see Fig. 4). The spiking thresholds were set when dV/dt exceeded 5 mV/ms. The interspike membrane potential was calculated when the dV/dt of the interspike membrane potential was 0 mV/ms.

Extracellular recordings in vivo. Extracellular recordings of Purkinje cell activity patterns were performed as described previously (Wulff et al., 2009). In short, 2- to 3-month-old WT and *Cacna1a*^{S218L} mice were immobilized using head-fixed pedestals constructed of stainless steel screws of 1 mm diameter equipped with custom-made connectors that were located in the frontal, medial, and temporal bones and embedded in dental acrylic. Craniotomies (~2 mm in diameter) were made in the occipital bone overlying (para-)vermal regions. Following a recovery period of ≥5 d we anesthetized the mice to place them in the restrainer following which we gradually canceled the isoflurane anesthesia (initial dose 1.5% in O_2) over a period of 5 min to prevent *Cacna1a*^{S218L} mice from seizing (van den Maagdenberg et al., 2010). The recovery from this anesthesia was monitored on electroencephalograms (EEGs) recorded from the motor and sensory cortices by means of the connectors attached to the screws within the pedestal. To prevent any possible contamination of the Purkinje cell recordings by the anesthesia, the extracellular recordings were started > 1 h after standard fast Fourier transform analysis of the EEG signals confirmed a full recovery (Hoebeek et al., 2010). Extracellular recordings were performed using borosilicate glass pipettes (2.0 mm outer diameter * 1.16 mm inner diameter) filled with 0.5 M NaCl of 4–8 MΩ, which were advanced into the cerebellum using a hydraulic manipulator (Trent Wells). During the recordings the openings in the skull were covered with saline, which was supplemented with 0.4 mM 1-EBIO where indicated. Recordings were subsequently amplified, filtered, and digitized using a CyberAmp (Axon Instruments) and CED1401 (CED), and were stored for off-line analysis using custom-written MATLAB (MathWorks) routines. Only single-unit Purkinje cell recordings (qualified as such by the presence of a clear climbing fiber pause following each complex spike; Wylie et al., 1995) of >60 s were analyzed using principal component waveform analysis (Eggermont, 1990). For each recording we analyzed the firing frequency of simple spikes and complex spikes, the CV of all intersimple spike intervals (ISSI), the CV2 of ISSIs, and the minimal climbing fiber pause. Distributions of ISSIs were normalized by dividing by maximal probability and using a 0.1 ms bin size. Burst-pause sequences were identified by a train of ≥10 simple spikes for which the ISSI gradually decreased to <5 ms followed by a consecutive pause in ISSIs of ≥25 ms. The length of the burst was calculated from the first simple spike after the previous burst-related pause to the last simple spike of the burst. The length of the pause was calculated from the last spike of the burst to the first following simple spike.

Behavioral analysis. Motor performance on the accelerating rotarod (range from 4 to 40 rpm, stepwise increments of 4 rpm every 30 s, maximal walking time 5 min) (model 7650; Ugo Basile Biological Research Apparatus) was measured every day in two trials with a 1 h intertrial interval in 2- to 3-month-old WT and *Cacna1a*^{S218L} mice. The indicated time ("latency to fall") is the time spent on the rotarod. Mice that made three consecutive rotations clamping on to the rotarod were scored as fallen.

Chlorzoxazone (CHZ; Sigma) was administered to the individually housed mice in drinking water as previously described (Alviña and Khodakhah, 2010). In short, the 15 mM CHZ solution supplemented with 0.1% hydroxypropyl-β-cyclodextrin (Tocris Bioscience) and 10% sucrose was prepared fresh every day. The pH was adjusted with 1 M NaOH to dissolve CHZ. Mice consumed on average 5.5 ml/d, which resulted in an estimated plasma concentration of ~30 μM (Alviña and Khodakhah, 2010). The weight of the animals and the extent of their water intake were monitored daily throughout the experiment and no significant changes were found.

Statistics. Statistical comparison between *Cacna1a*^{S218L} mutants and WT littermates was performed using paired or unpaired, two-tailed Student's t test or repeated-measures ANOVA, with $p < 0.05$ defining a significant difference. Summarized data are represented as mean ± SEM. The number of measurements per experiment indicates the number of neurons recorded, unless stated otherwise.

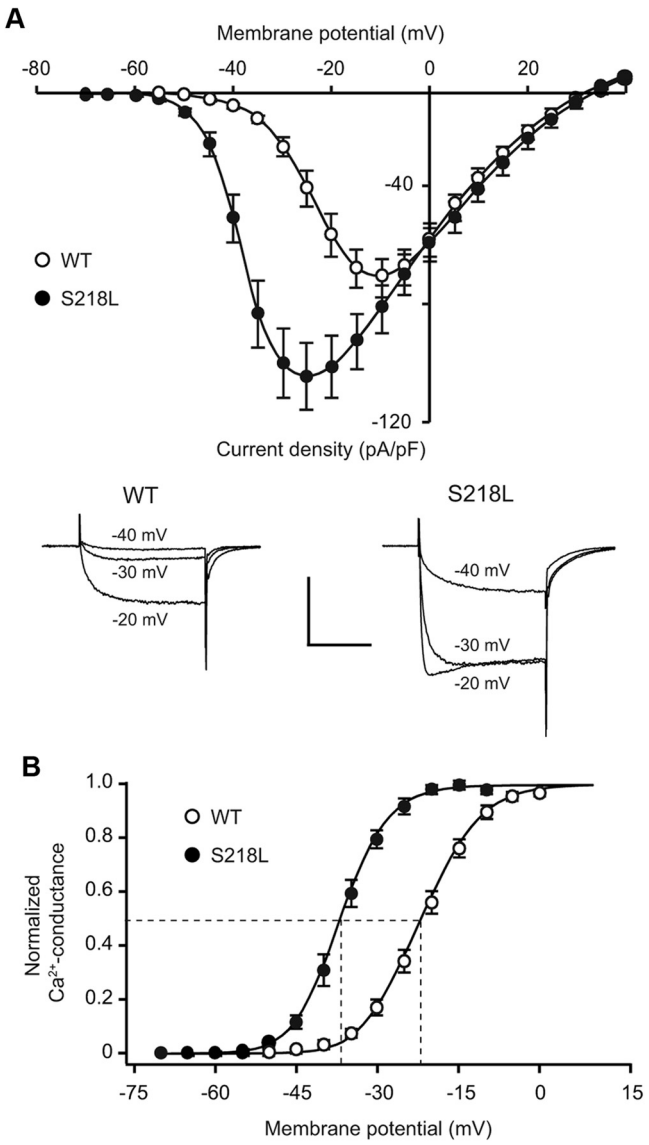

Figure 1. Negative shift of voltage–current relationships of whole-cell Ca^{2+} currents in acutely dissociated *Cacna1a*^{S218L} Purkinje cells. ***A***, Voltage–current relationship of Ca^{2+}-current densities relative to membrane potentials in acutely dissociated WT Purkinje cells ($n = 10$) and *Cacna1a*^{S218L} Purkinje cells ($n = 10$). Insets show representative traces of Ca^{2+} currents in WT and *Cacna1a*^{S218L} Purkinje cells evoked by 50 ms depolarizing pulses to −40, −30, and −20 mV (holding potential = −70 mV). Scale bars: vertical, 75 pA/pF; horizontal, 20 ms. ***B***, Accompanying normalized Ca^{2+} conductance at different depolarizing voltages in WT and *Cacna1a*^{S218L} Purkinje cells. Solid curves indicate Boltzmann fits and dashed lines indicate corresponding voltages of half-maximum conductance (p values indicated in Results).

Results

Altered $Ca_V2.1$-mediated Ca^{2+} influx in *Cacna1a*^{S218L} Purkinje cells

We first studied the effect of the S218L mutation in the *Cacna1a* gene, which induces an increased channel opening probability and Ca^{2+} influx (Tottene et al., 2005; van den Maagdenberg et al., 2010), on $Ca_V2.1$-channel function in Purkinje cells. We recorded whole-cell Ca^{2+}-current densities in acutely dissociated Purkinje cells from P16–P21 *Cacna1a*^{S218L} mutants and WT littermates. In WT Purkinje cells the threshold for inward Ca^{2+} currents was -44 ± 2 mV and the peak (-67.3 ± 6.3 pA/pF) was detected at -10 mV, whereas in *Cacna1a*^{S218L} Purkinje cells the threshold was -56 ± 2 mV ($p < 0.001$ compared with WT) and the peak (-103.5 ± 12.1 pA/pF) was detected at -25 mV (Fig. 1*A*). To quantify the effect of the mutation on voltage-dependent activation, we determined the normalized whole-cell conductance at each membrane potential and fitted the data to a Boltzmann function. In *Cacna1a*^{S218L} Purkinje cells the voltages of half-maximal conductance ($V_{1/2}$) was significantly more hyperpolarized than in WT Purkinje cells (-36.4 ± 1.2 mV vs -21.2 ± 1.5 mV, respectively; $p < 0.001$) (Fig. 1*B*). The prominence of this shift can be appreciated by considering the larger current density in *Cacna1a*^{S218L} neurons upon relatively mild depolarization (e.g., at –30 mV the currents in *Cacna1a*^{S218L} Purkinje cells are five times greater than in WT Purkinje cells).

To confirm that the negative shift in the voltage dependence of Purkinje cell Ca^{2+} currents is due to affected $Ca_V2.1$-channel functioning rather than concurrent alterations of other types of VGCCs (Mintz et al., 1992), we next recorded Ca^{2+} currents in WT and *Cacna1a*^{S218L} Purkinje cells in the presence of $Ca_V2.1$-channel blocker ω-Agatoxin-IVA. Bath application of 0.2 μM ω-Agatoxin-IVA indeed canceled the left-shift in activation threshold of Ca^{2+} current (peak: WT: -7.5 ± 1.1 pA/pF at -10 mV; *Cacna1a*^{S218L}: -7.1 ± 1.4 pA/pF at -10 mV; $p = 0.38$; $V_{1/2}$: WT: -26.4 ± 1.8 mV; *Cacna1a*^{S218L}: -26.3 ± 3.0 mV; $p = 0.75$). The fact that the remaining Ca^{2+} currents are not different in WT suggests a lack of compensatory changes in Ca^{2+} currents mediated by non-P/Q-type VGCCs in *Cacna1a*^{S218L} Purkinje cells. Together these findings indicate that $Ca_V2.1$ channels in *Cacna1a*^{S218L} Purkinje cells open in response to depolarizations that are insufficient to activate $Ca_V2.1$ channels in WT Purkinje cells, which confirms the negative-shifts of $Ca_V2.1$ currents in cerebellar granule cells of *Cacna1a*^{S218L} mice (van den Maagdenberg et al., 2010).

Irregular spontaneous action potential firing in *Cacna1a*^{S218L} Purkinje cells

To test how the shift in channel activation could affect Purkinje cell spiking patterns, we recorded the spontaneous firing patterns of Purkinje cells in acutely prepared cerebellar slices in the presence of blockers for synaptic (i.e., glutamatergic and GABAergic) transmission. Under these conditions, Purkinje cell spiking activity appeared continuous and regular in all recorded WT cells, whereas all *Cacna1a*^{S218L} Purkinje cells showed an intermittent firing pattern in which periods of tonic firing (27.8 ± 6.1 s) were interrupted by bursting activity (35.3 ± 9.5 s) during which the amplitude of the spikes reduced (Fig. 2*A*). The average firing frequency of *Cacna1a*^{S218L} Purkinje cell activity was lower, whereas their irregularity, as measured by the CV and CV2 (see also Material and methods) (Holt et al., 1996), was higher (all p values <0.003) (Fig. 2*B*). These differences between mutants and WTs also held when we analyzed the tonic and burst-pause firing periods of *Cacna1a*^{S218L} Purkinje cells separately; the firing frequencies during both tonic and burst-pause firing phases were lower than those of WT, whereas CV and CV2 values were significantly higher (all $p < 0.01$) (Fig. 2*B*).

To study the potential impact of synaptic inputs on Purkinje cell action potential firing, we also performed loose-cell attached

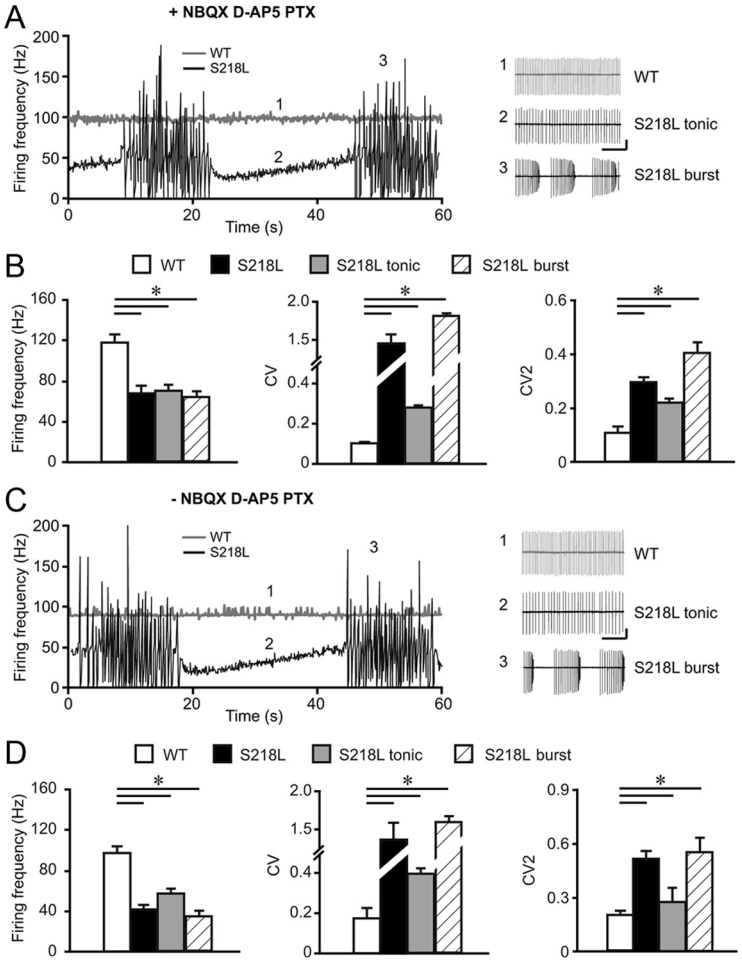

Figure 2. Irregular intrinsic activity of *Cacna1a*^{S218L} Purkinje cells. ***A***, Moving averages (bin width 100 ms) of the firing frequency of intrinsic Purkinje cell activity in WT (gray line) and *Cacna1a*^{S218L} (black line) Purkinje cells in the presence of blockers for glutamatergic (NBQX, 10 μM; D-AP5, 10 μM) and $GABA_A$-mediated synaptic transmission (PTX, 100 μM). The numbers 1 and 2 indicate the time points at which the continuous firing in the WT (top inset) and *Cacna1a*^{S218L} Purkinje cell (middle inset) occurred, and the number 3 indicates burst firing in the *Cacna1a*^{S218L} Purkinje cell (lower inset). Scale bars: vertical, 50 pA; horizontal, 200 ms. ***B***, The firing frequency, CV, and CV2 values of intrinsic activities from WT ($n = 15$) and *Cacna1a*^{S218L} ($n = 14$) Purkinje cells. The frequency, CV, and CV2 values during tonic and burst firing episodes are calculated separately. ***C***, Similar as in ***A*** in the absence of blockers of glutamatergic and $GABA_A$-mediated synaptic transmission. ***D***, Similar as in ***B*** in the absence of blockers of glutamatergic and $GABA_A$-mediated synaptic transmission (WT, $n = 18$; *Cacna1a*^{S218L}, $n = 16$). Asterisks indicate significant differences (p values indicated in Results).

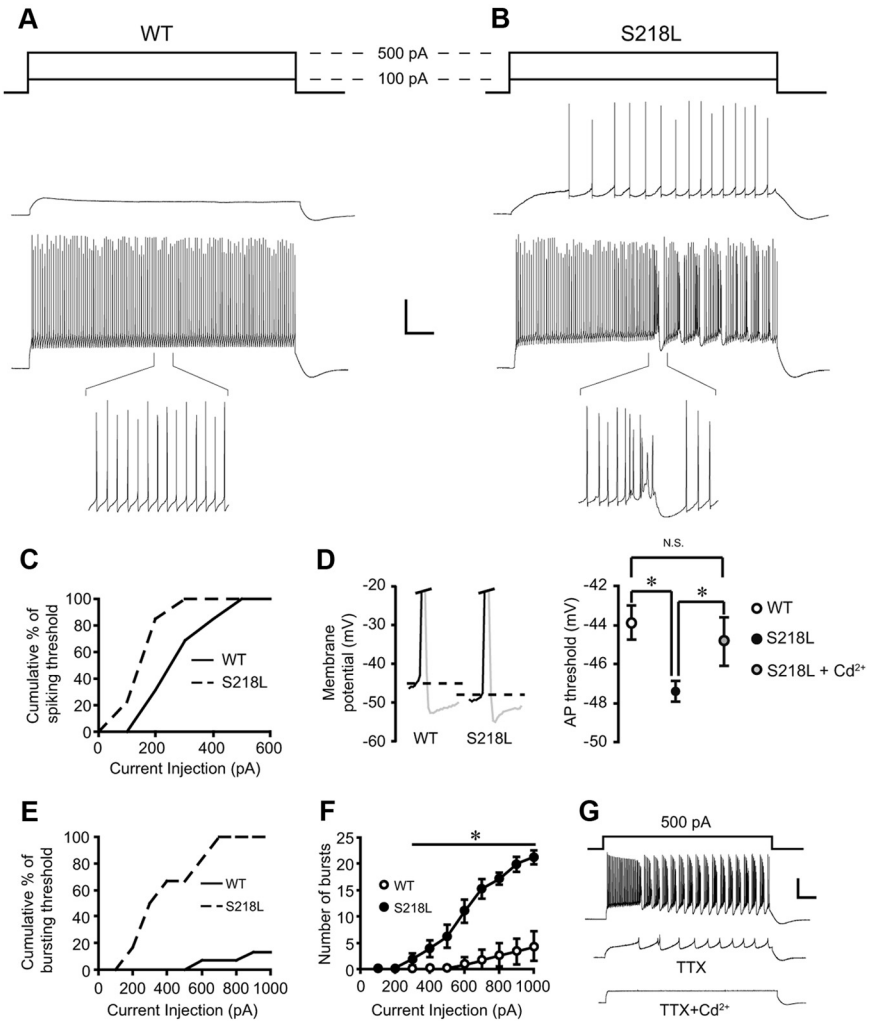

Figure 3. More negative thresholds for action potentials and Ca^{2+} spikes in *Cacna1a*^{S218L} Purkinje cells. ***A***, ***B***, Samples of WT (***A***) and *Cacna1a*^{S218L} (***B***) Purkinje cell responses to 1500 ms depolarizing current pulses ranging from 100 to 1000 pA relative to the bias current to clamp the membrane potential to −65 mV. Scale bars: vertical, 20 mV; horizontal, 150 ms. Bottom, WT Purkinje cells show regular action potential firing for 1500 ms, whereas *Cacna1a*^{S218L} Purkinje cell show occasional Ca^{2+} spike firing. ***C***, Cumulative percentage of spiking thresholds plotted against the injected currents in WT ($n = 13$) and *Cacna1a*^{S218L} ($n = 13$) Purkinje cells. The percentage indicates the ratio of spiking Purkinje cells over the total number of recorded Purkinje cells at a given level of current injection. ***D***, Left, Representative examples of action potentials from WT and *Cacna1a*^{S218L} Purkinje cells. Horizontal lines indicate the action potential threshold. Right, Mean action potential (AP) threshold in WT ($n = 13$) and *Cacna1a*^{S218L} ($n = 13$) Purkinje cells in normal ACSF and in *Cacna1a*^{S218L} Purkinje cells in presence of 100 μM Cd^{2+} to block all VGCCs ($n = 8$). ***E***, ***F***, Cumulative percentage of Purkinje cells firing bursts (***E***) and the mean number of bursts (***F***) in response to 1500 ms current injections of 100–1000 pA for WT ($n = 13$) and *Cacna1a*^{S218L} ($n = 13$) Purkinje cells. The percentage indicates the ratio of bursting Purkinje cells over the total number of recorded Purkinje cells at a given level of current injection. ***G***, Top, Sample of *Cacna1a*^{S218L} Purkinje cell responses to 1500 ms current injections of 500 pA depolarizing current relative to the bias current to clamp the membrane potential to −65 mV in normal ACSF. Middle, After application of 1 μM TTX. Bottom, After coapplication of 1 μM TTX and 100 μM Cd^{2+}. Scale bars: vertical, 20 mV; horizontal 150 ms. Asterisks indicate significant differences (*p* values indicated in Results).

recordings in absence of blockers of synaptic transmission. Under these conditions, we found a similar disruption of action potential firing patterns in *Cacna1a*^{S218L} Purkinje cells: intermittent tonic and burst-pause firing occurred in 10 of 16 recordings and six cells exclusively showed burst-pause sequences (Fig. 2*C*). On average we found that the firing frequency was lower and that CV as well as CV2 values were higher (all p values < 0.03). Similarly, also during tonic firing and during burst-pause firing the frequency was reduced and the irregularity was increased (all p values < 0.03) (Fig. 2*D*). Thus, the Purkinje cell firing pattern in *Cacna1a*^{S218L} mutants remains defective under the influence of synaptic inputs.

Hyperexcitability of somatic action potential and dendritic Ca^{2+} spike firing in *Cacna1a*^{S218L} Purkinje cells

To study the intrinsic excitability of Purkinje cells we next tested their responses to somatic current injections. *Cacna1a*^{S218L} Purkinje cells fired action potentials in response to the lowest current injection tested, i.e., 100 pA relative to the holding current, whereas WT Purkinje cells did not ($p < 0.005$) (Fig. 3, *A–C*). In addition, *Cacna1a*^{S218L} Purkinje cells showed a more negative interspike membrane potential ($p < 0.03$) and a more negative action potential initiation threshold ($p < 0.001$); but the action potential rise time, amplitude, and decay time constant as well as the basic membrane properties were not significantly different from WT (Fig. 3*D*; Table 1; see also Fig. 7*D*). The more negative action potential initiation threshold is likely related to the activation of VGCC, because bath application of the global VGCC blocker Cd^{2+} (100 μM) canceled the significant difference in action potential threshold ($p = 0.01$ relative to *Cacna1a*^{S218L} and $p = 0.77$ relative to WT) (Fig. 3*D*).

In addition, somatic current injections into *Cacna1a*^{S218L} Purkinje cells readily evoked burst episodes, which consisted of a high-frequency train of action potentials and a slower depolarization (Fig. 3*B*): at 300 pA 6 of 13 *Cacna1a*^{S218L} Purkinje cells fired such bursts and at

Table 1. Action potential kinetics and passive Purkinje cell properties

	AP amplitude (mV)	HW (ms)	*dV/dt* (V/s)	−*dV/dt* (V/s)	IMP (mV)	τ_{decay} (ms)
WT	69.9 ± 2.2	0.22 ± 0.01	397 ± 20	343 ± 14	−48.0 ± 0.7	11.1 ± 0.4
S218L	66.3 ± 1.6	0.22 ± 0.01	400 ± 22	369 ± 14	−50.4 ± 0.8	10.3 ± 0.4
t test	0.22	0.96	0.93	0.21	0.03	0.64

Absolute amplitude of action potential (AP); half-width (HW) (ms) of AP; maximum rising slope (*dV/dt*) (V/s); maximum repolarizing slope (−*dV/dt*) (V/s); interspike membrane potential (IMP), and decay time constant (τ_{decay}) of the membrane capacitance calculated from 19 WT and 18 *Cacna1a*^{S218L} Purkinje cells.

600 pA all 13 *Cacna1a*^{S218L} Purkinje cells fired bursts. In contrast, none of the WT neurons showed burst activity at 300 pA, and 2 of 13 WT neurons fired similar burst activity in response to somatic current injections of ≥600 pA ($p < 0.001$) (Fig. 3*E*,*F*). To unravel the role of Na^+- and Ca^{2+}-channel activity in these burst episodes we repeated the somatic current injections in the presence of 1 μM TTX, which canceled action potential firing. Yet, the slower depolarization related to the burst episode was only blocked when we subsequently applied 100 μM Cd^{2+}, which blocks all VGCCs (Fig. 3*G*).

Previous studies identified similar burst-like activity in Purkinje cells as dendritic events that are mediated by widespread activation of $Ca_V2.1$ channels (Hounsgaard and Yamamoto, 1979; Llinás and Sugimori, 1980a,b; Stuart and Häusser, 1994; Kitamura and Häusser, 2011). We examined the dendritic excitability of *Cacna1a*^{S218L} Purkinje cells using simultaneous somatic and dendritic whole-cell recordings (cf. Material and Methods) (Fig. 4*A*). The spontaneously occurring Ca^{2+}-spike activity was initiated by dendritic depolarization of 5.2 ± 1.3 mV relative to the membrane potential during the previous ISI (cf. Material and Methods) and was consistently followed by a somatic depolarization (Fig. 4*A*). When we injected 300 pA or more depolarizing current through the dendritic recording pipette, Ca^{2+} spikes could be readily elicited in *Cacna1a*^{S218L} Purkinje cells, whereas in none of the WT Purkinje cells were we able to elicit Ca^{2+}-spike activity using current injections up to 1 nA (Fig. 4*B*,*C*). The amplitude of the evoked dendritic Ca^{2+} spikes was not correlated to the location of the dendritic recording electrode (correlation coefficient = −0.09, $R^2 = 0.001$) (Fig. 4*D*). Since dendritic current injections >2 nA have been shown to evoke Ca^{2+}-spike activity in WT Purkinje cells (Rancz and Häusser, 2006), our data indicate that in *Cacna1a*^{S218L} Purkinje cells the induction threshold for dendritic burst firing is reduced.

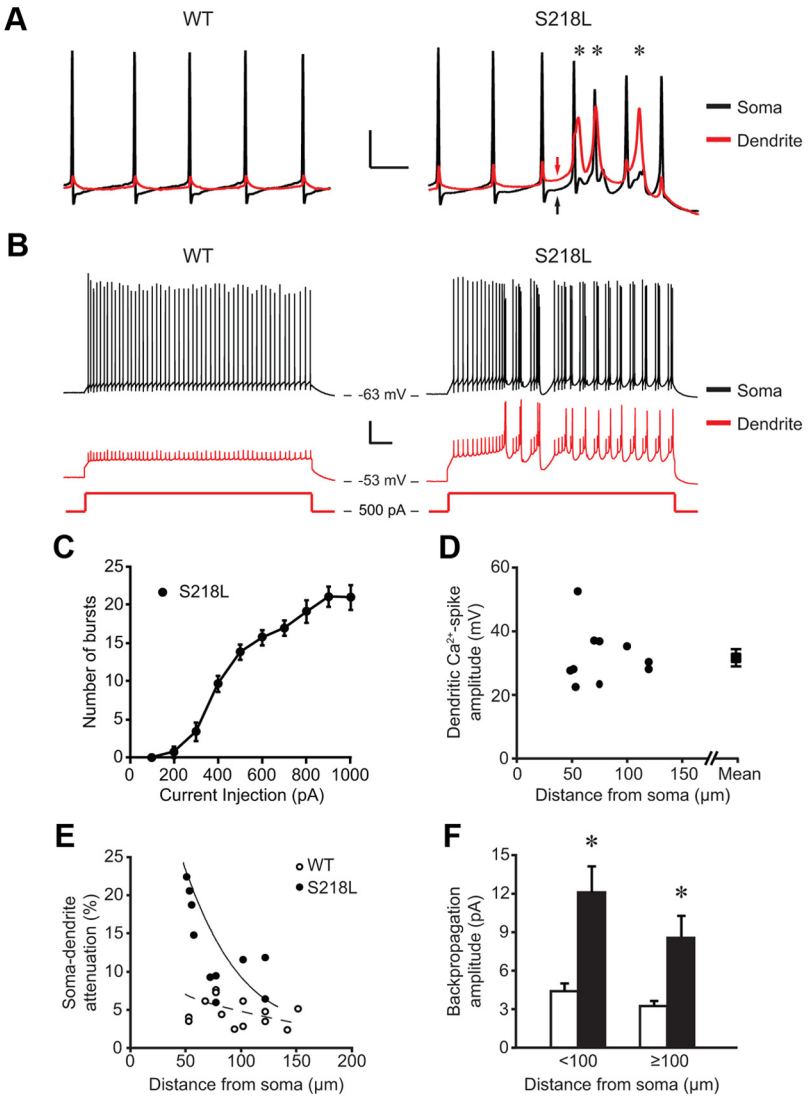

Figure 4. Dendritic Ca^{2+} spikes and reduced attenuation of somatic action potentials in *Cacna1a*^{S218L} Purkinje cell dendrites. ***A***, Typical somatic (top, black) and dendritic (bottom, red; recorded 75 μm from the soma) membrane potentials in WT (left) and *Cacna1a*^{S218L} (right) Purkinje cell. Note the severe attenuation of the somatic action potentials in the WT dendrite but to a lesser extent in the *Cacna1a*^{S218L} Purkinje cell. Scale bars: vertical, 20 mV; horizontal 10 ms. Arrows indicate a rise of dendritic membrane potential that consistently precedes the burst firing. ***B***, Dendritic current injections of 500 pA into the dendrite for 1 s resulted in tonic action potential firing in WT Purkinje cells, but evoked dendritic Ca^{2+} spikes in *Cacna1a*^{S218L} Purkinje cells. Scale bars: vertical, 20 mV; horizontal, 100 ms. ***C***, Distribution of the number of evoked Ca^{2+} spikes relative to the current injected into the Purkinje cell dendrite. ***D***, Maximal dendritic membrane potential during spontaneously occurring Ca^{2+} spikes specified for various distances from the soma. The average maximal dendritic potential is represented as "mean" (square). Correlation coefficients are indicated in Results. ***E***, Attenuation (indicated as the ratio of dendritic and somatic amplitudes) of somatically generated action potentials quantified per distance of the dendritic patch electrode from the soma. ***F***, Averaged amplitude of dendritic potentials for distances < 100 μm (WT $n = 7$ and *Cacna1a*^{S218L} $n = 7$) and ≥ 100 μm (WT $n = 6$ and *Cacna1a*^{S218L} $n = 3$). Asterisks indicate significant differences (p values indicated in Results).

The dual somatic–dendritic recordings also enabled us to quantify the dendritic spread of the membrane depolarization evoked by somatic action potentials. Although we found that in both WT and *Cacna1a*^{S218L} Purkinje cells this amplitude was correlated to the distance from the soma (WT: correlation coefficient = −0.35, $R^2 = -0.21$; *Cacna1a*^{S218L}: correlation coefficient = −0.66, $R^2 = -0.58$), the attenuation of the dendritic membrane depolarization evoked by somatic action potentials in *Cacna1a*^{S218L} Purkinje cells was decreased compared with WT Purkinje cells in both proximal (<100 μm from the soma) and distal dendrites (>100 μm from the soma) (all p values <0.003) (Fig. 4*E*,*F*). Together these results not only show that the S218L mutation shifts the activation threshold for somatic action potentials and dendritic Ca^{2+} spikes to more negative membrane potentials, but also that somatic action potentials are more effective in depolarizing the Purkinje cell dendritic tree.

PF output elicits burst-like activity in *Cacna1a*^{S218L} Purkinje cells

The dendritic hyperexcitability of *Cacna1a*^{S218L} Purkinje cells is a potential source of disrupted simple spike firing patterns in that it potentially disrupts postsynaptic responses evoked by synaptic

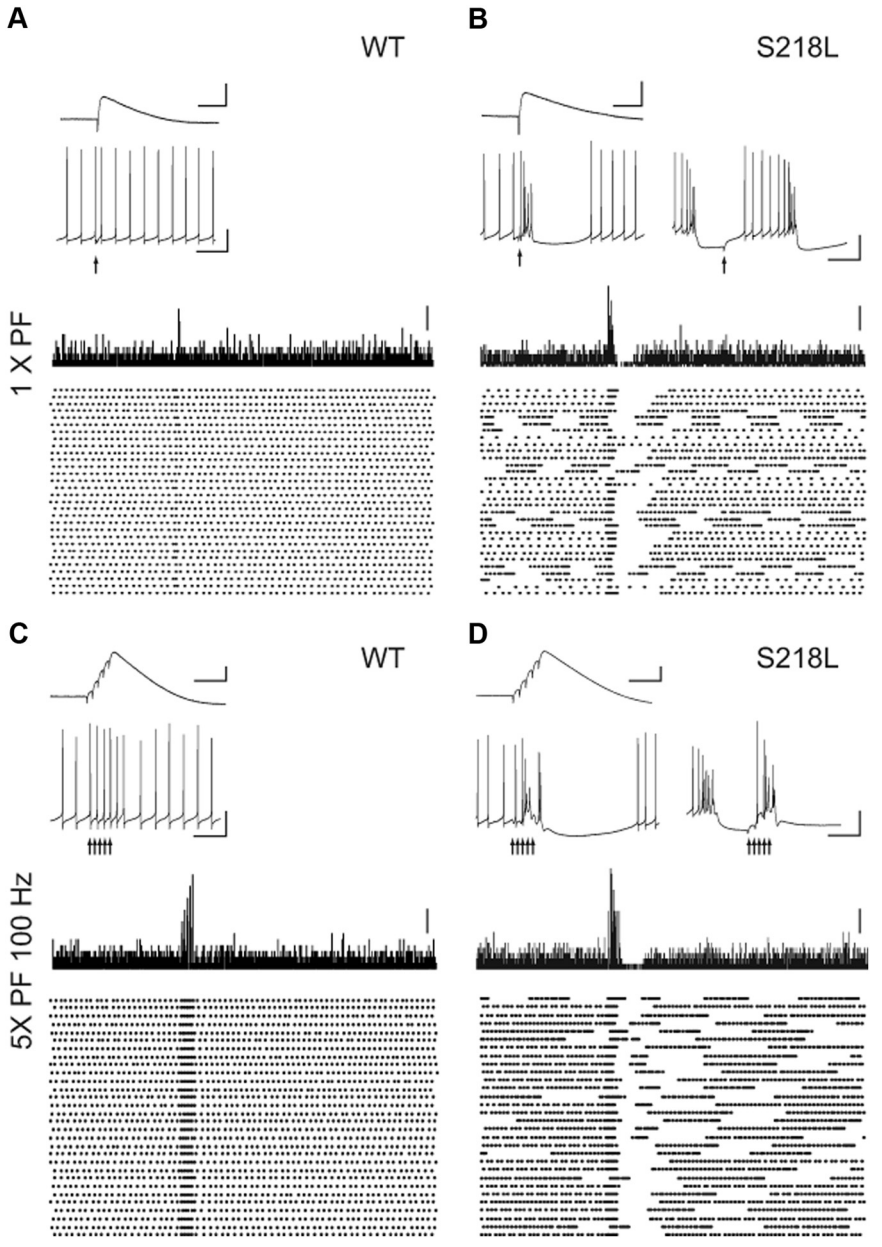

Figure 5. PF stimulation induces Ca^{2+} spikes in *Cacna1a*^{S218L} Purkinje cells. ***A***, Top, Representative traces of 2 mV PF-EPSPs (top inset; scale bars: vertical, 2 mV; horizontal 50 ms) recorded when the Purkinje cell membrane potential was clamped at −70 mV. Accompanying Purkinje cell spiking patterns in response to the same PF stimulus were recorded without holding current (bottom inset; scale bars: vertical, 20 mV; horizontal 50 ms). Vertical arrow indicates time of stimulus. Bottom, Histogram of spike counts and accompanying raster plot of 30 repeats of a single PF stimulus. Scale bar: 4 spike counts. ***B***, Similar to ***A*** for a typical *Cacna1a*^{S218L} Purkinje cell that showed intermittent continuous and burst-pause sequences. Bottom insets show representative responses to a single PF stimulus while the neuron fired continuously (left) or burst-like (right) before the stimulus. Note that when the *Cacna1a*^{S218L} Purkinje cell fired continuously, single PF-EPSP induced a burst, whereas when the Purkinje cell fired bursts the PF-EPSP depolarized the membrane potential to reset the burst-pause sequence. ***C***, ***D***, Similar to ***A***, ***B*** for a 100 Hz train of 5 PF stimuli. ***C***, WT Purkinje cells respond with an action potential to each individual PF stimulus in the train (bottom inset). Scale bars: (for PF-EPSP) vertical 4 mV, horizontal 50 ms; (for action potential) vertical 20 mV, horizontal 50 ms; (for histogram) 4 spike counts. ***D***, *Cacna1a*^{S218L} Purkinje cells always responded with a burst to the PF train stimulus, regardless of the prestimulus firing pattern.

inputs. To study the effect of the PF to Purkinje cell input, we evoked ~2 mV postsynaptic potentials by electrical stimulation of the molecular layer surrounding the recorded Purkinje cells in the presence of 100 μM PTX to block $GABA_A$-mediated inhibitory transmission. In the absence of somatic current injections, we found that this single, amplitude-controlled PF stimulation resulted in one well timed action potential in all 12 WT Purkinje cells, but elicited a burst-pause sequence in 12 of 13 *Cacna1a*^{S218L} Purkinje cells (Fig. 5*A*,*B*). The average burst and pause sequence consisted of 6.4 ± 1.3 action potentials and a 186.6 ± 25.6 ms pause. In the *Cacna1a*^{S218L} Purkinje cells that were in a burst-like firing state (Fig. 2*A*) at the time of the stimulation, the postsynaptic potential appeared to reset the burst-pause cycle (Fig. 5*B*). This difference between WT and *Cacna1a*^{S218L} Purkinje cells in response to PF stimuli persisted when we applied a 100 Hz stimulus train of five pulses (Jörntell and Ekerot, 2006) (Fig. 5*C*,*D*). All WT cells responded to each PF-EPSP in the train with a well timed action potential, whereas in all *Cacna1a*^{S218L} Purkinje cells the train stimuli consistently induced bursts, regardless of the preceding activity pattern. These data indicate that *Cacna1a*^{S218L} Purkinje cells are hyperexcitable to such an extent that even granule cell input elicits dendritic Ca^{2+} spikes and subsequent pauses.

Effects of the negative-shift in $Ca_V2.1$ voltage dependence on SK currents

In cerebellar Purkinje cells the effect of VGCCs on the excitability is closely related to activation of Ca^{2+}-dependent K^+ channels. For instance, it has been shown that the reduced $Ca_V2.1$-mediated Ca^{2+} influx in *tottering*, *ducky,* and *leaner* Purkinje cells evokes irregular somatic action potential firing by means of reduced SK-channel activation (Walter et al., 2006). To test the effect of the negative shift in the voltage dependence of $Ca_V2.1$ channels in *Cacna1a*^{S218L} Purkinje cells on the activation of SK-channels, we recorded tail currents following Ca^{2+} influx evoked by various holding potentials in dissociated Purkinje cells. Under the conditions used (cf. Material and Methods), the tail currents are known to be indicative of SK-channel activity (Cingolani et al., 2002). The activation curve of these SK currents showed a significant negative shift in *Cacna1a*^{S218L} Purkinje cells relative to those in WT ($V_{1/2}$ in *Cacna1a*^{S218L} −41.9 ± 0.1 mV vs WT −30.6 ± 0.6 mV; $p < 0.001$) (Fig. 6*A*) without a significant change in maximal SK-current amplitude ($p = 0.69$). The negative shift in SK-activation curve is comparable to the negative shift in the Ca_V-activation curve (Fig. 6*B*). In fact, the ratio between Ca_V and SK currents (cf. Material and Methods) was not significantly different in *Cacna1a*^{S218L} Purkinje cells (all p values >0.15) (Fig. 6*B*). Even at membrane potentials more hyperpolarized than −40 mV, i.e., potentials at which $Ca_V2.1$ channels only in *Cacna1a*^{S218L} Purkinje cells are activated no significant increase in the ratio between Ca_V- and SK-current densities was found.

In addition to the direct assessment of the ratio between Ca_V- and SK-current densities, also the amplitude of the afterhyperpolarization (AHP) relative to the action potential threshold is indicative of SK activity. As expected, we also found that the AHP amplitude in *Cacna1a*^{S218L} Purkinje cells was not significantly different from that in WT ($p = 0.26$) (Fig. 6*C*). These results indicate that in *Cacna1a*^{S218L} Purkinje cells SK channels are activated at more negative membrane potentials in response to the negative shift of the $Ca_V2.1$ activation.

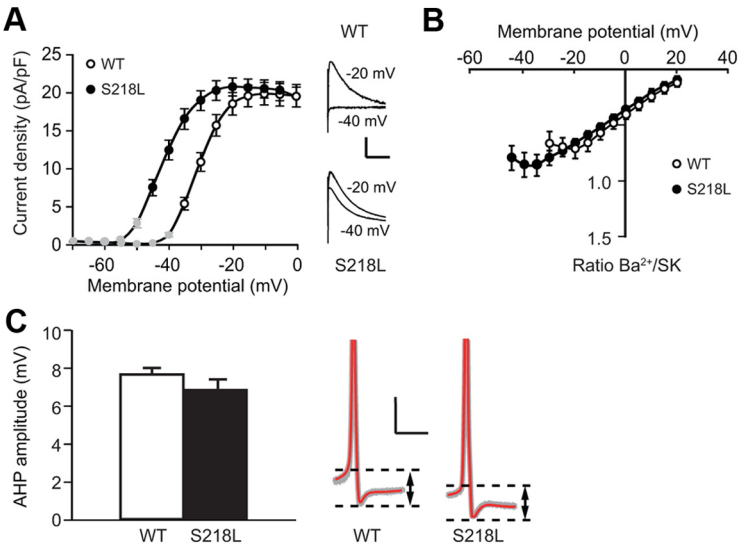

Figure 6. Concurrent left shift of SK-channel activation in *Cacna1a*^{S218L} Purkinje cells. ***A***, Current–voltage relationship of SK currents in WT ($n = 18$) and *Cacna1a*^{S218L} ($n = 20$) isolated Purkinje cell somata. Peak tail current densities were plotted against depolarizing voltages. Insets show representative traces of tail currents in WT and *Cacna1a*^{S218L} Purkinje cells evoked by 50 ms depolarizing pulses to −40 and −20 mV (holding potential = −70 mV). Scale bars: vertical, 10 pA/pF; horizontal, 20 ms. Note that masked data points (current density < 5 pA/pF) are not considered for further analysis. ***B***, Ratio of Ba^{2+} and SK currents at various voltages in WT ($n = 9$) and *Cacna1a*^{S218L} ($n = 8$) Purkinje cells. ***C***, Mean AHP amplitude in WT ($n = 13$) and *Cacna1a*^{S218L} ($n = 13$) Purkinje cells in acute cerebellar slices. Representative examples of the AHP amplitude (indicated by dashed lines and arrows) of 10 action potentials (gray) from a single WT and a single *Cacna1a*^{S218L} Purkinje cell and their average (red). Scale bars: vertical, 10 mV; horizontal, 2 ms. Note that action potentials have been clipped for clarity of representation.

Involvement of SK channels in modulating dendritic Ca^{2+} spike activity in *Cacna1a*^{S218L} Purkinje cells

Given that enhancing the SK channel function improves Purkinje cell firing regularity in mutant mice characterized by decreased $Ca_V2.1$-mediated Ca^{2+} influx (Walter et al., 2006; Alviña and Khodakhah, 2010), we hypothesized that reducing SK channels might improve Purkinje cell firing regularity in the *Cacna1a*^{S218L} mutants. To test this hypothesis we applied the SK-channel blocker apamin to cerebellar slices of the *Cacna1a*^{S218L} mutants. Surprisingly, bath application of apamin (range: 0.1 nM to 5 μM) did not restore the disrupted spiking pattern in *Cacna1a*^{S218L} Purkinje cells. In fact, each concentration of apamin severely disrupted the continuous action potential firing (Fig. 7*A*,*B*) and decreased the threshold of dendritic Ca^{2+} spikes in both WT and *Cacna1a*^{S218L} Purkinje cells (Fig. 7*C*,*D*). Given that this SK-channel blocker seemed to worsen the disruption of Purkinje cell firing we next reasoned that by promoting the SK-channel function we might be able to reduce the effects of the S218L mutation on Purkinje cell firing. Indeed, bath application of the SK-channel activator 1-EBIO (10 μM) not only significantly raised the action potential threshold and burst threshold of *Cacna1a*^{S218L} Purkinje cells to values not significantly different from WT (all $p > 0.15$) (Fig. 7*A–D*), but it also enhanced the AHP amplitude relative to the action potential threshold (-6.9 ± 0.6 mV relative to 9.7 ± 0.8 mV; $p = 0.001$) (Devor et al., 1996; Pedarzani et al., 2001; Walter et al., 2006) without affecting the input resistance ($p > 0.45$) (Fig. 7*E*). Hence, in our *in vitro* preparation 1-EBIO enhanced the SK-channel function and counteracted the hyperexcitability of *Cacna1a*^{S218L} Purkinje cells.

In vitro application of SK activators reduces occurrence of burst-pause sequences in *Cacna1a*^{S218L} Purkinje cell activity

Since 1-EBIO counteracts the hyperexcitability of *Cacna1a*^{S218L} Purkinje cells to current injections, we next tested the effects of SK-channel activators on Purkinje cell spontaneous action potential firing. Bath application of either 10 μM 1-EBIO or 60 μM CHZ (Alviña and Khodakhah, 2010) effectively inhibited the burst-like firing patterns in all *Cacna1a*^{S218L} Purkinje cells (S218L + 1-EBIO: $n = 7$; S218L + CHZ: $n = 8$) (Fig. 8*A*,*B*), which significantly improved the regularity of Purkinje cell firing compared with nontreated *Cacna1a*^{S218L} Purkinje cells (p values for both CV and CV2 < 0.05). Both 1-EBIO and CHZ also decreased the tonic firing frequency of *Cacna1a*^{S218L} Purkinje cells ($p < 0.05$). Thus, both 1-EBIO and CHZ show a potent effect on SK-channel function in *Cacna1a*^{S218L} Purkinje cells, which indicates that the effects of the S218L mutation do not saturate the dynamic range of SK-channel function.

Disrupted Purkinje cell firing in alert *Cacna1a*^{S218L} mice and the effect of a SK-channel activator

Purkinje cells in alert *Cacna1a*^{S218L} mutants showed qualitatively normal simple spike and complex spike waveforms (Fig. 9*A*), but the overall activity pattern was severely disrupted. The most predominant caveat in *Cacna1a*^{S218L} simple spike firing was the occurrence of long pauses (Fig. 9*B*): on average, $4.5 \pm 0.7\%$ of all ISSIs lasted ≥ 100 ms, which is significantly more than in WT ($0.03 \pm 0.02\%$; $n = 14$; $p < 0.001$) and resulted in a significantly lower firing frequency in *Cacna1a*^{S218L} Purkinje cells ($n = 25$; $p < 0.001$) (Fig. 9*C*). Also, the pauses in simple spike firing following each complex spike were significantly prolonged in *Cacna1a*^{S218L} Purkinje cells ($p < 0.001$) (Fig. 9*D*). Surprisingly, the burst-pause sequences as recorded in all *Cacna1a*^{S218L} Purkinje cells in our *in vitro* preparation (Fig. 2) occurred in only 4 of 25 mutant cells recorded *in vivo* (Fig. 9*B*). On average, these four recordings showed burst-pause sequences during $3.5 \pm 1.3\%$ of the recorded time. The bursts lasted for 320 ± 88 ms and the pauses 238 ± 75 ms. None of the WT Purkinje cell recordings showed similar burst-pause sequences. Overall, we quantified the irregularity of simple spike firing patterns by calculating the CV and CV2 values per recording. Both values were significantly increased in *Cacna1a*^{S218L} Purkinje cells compared with WT Purkinje cells (all p values < 0.02) (Fig. 9*C*). In contrast to this disrupted simple spike firing pattern, both the firing frequency and the regularity of complex spikes were not affected in *Cacna1a*^{S218L} Purkinje cells (all p values > 0.4) (Fig. 9*D*). Together these extracellular recordings show that both the firing frequency and the regularity of Purkinje cell simple spike firing are abnormal in ataxic *Cacna1a*^{S218L} mice.

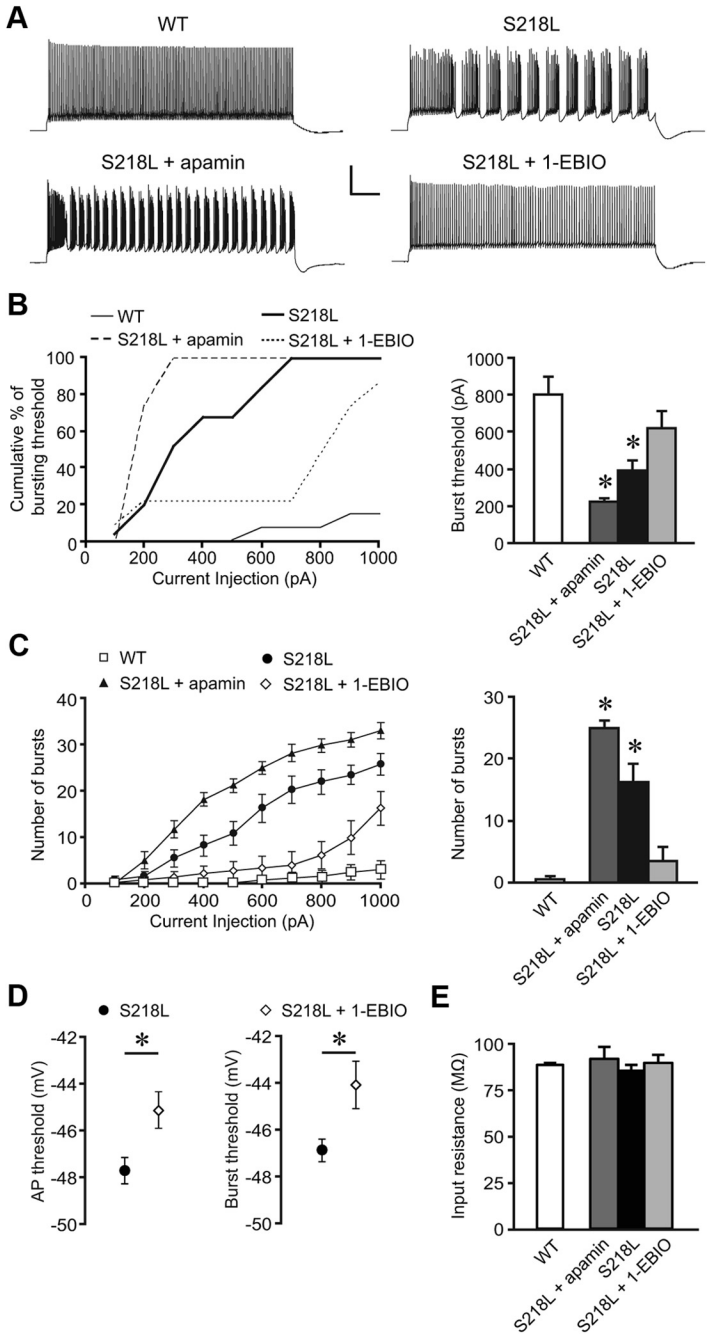

Figure 7. SK-channel activator 1-EBIO increases the thresholds for somatic action potentials and dendritic Ca^{2+} spikes in *Cacna1a*^{S218L} mice. ***A***, Representative traces of Purkinje cell firing patterns of WT, *Cacna1a*^{S218L}, *Cacna1a*^{S218L} + apamin (0.5 nM), and *Cacna1a*^{S218L} + 1-EBIO (10 μM) in response to 1500 ms depolarizing current pulses of 500 pA relative to the bias current to clamp the membrane potential to −65 mV. Scale bars: vertical, 20 mV; horizontal, 150 ms. ***B***, Left, Cumulative percentage of bursting thresholds in response to 1500 ms current injections of 100–1000 pA plotted against the injected currents in *Cacna1a*^{S218L} Purkinje cells with 0.5 nM apamin ($n = 7$) or in *Cacna1a*^{S218L} Purkinje cells with 10 μM 1-EBIO in the bath ($n = 8$). The percentage indicates the ratio of bursting Purkinje cells over the total number of recorded Purkinje cells at a given level of current injection. For comparison the WT and *Cacna1a*^{S218L} Purkinje cell data are represented again (as in Fig. 3*E*). Right, Averaged bursting threshold for the four groups represented on the left. Note that only the *Cacna1a*^{S218L} + 1-EBIO values did not differ significantly from the WT group. ***C***, Left, Similar groups as in ***B***, but now representing the mean number of bursts during the 1500 ms current injection. Right, The average number of bursts at 600 pA of current injection. Note that application of apamin increases the bursting activity, whereas 1-EBIO inhibits the bursting activity. Also note that only the *Cacna1a*^{S218L} + 1-EBIO values did not differ significantly from the WT group. ***D***, The effects of 1-EBIO on the average action potential threshold (left) and Ca^{2+}-burst threshold (right) in *Cacna1a*^{S218L} cells with and without 1-EBIO. ***E***, The average input resistances of all cells presented in (***B–D***) as recorded in voltage-clamp mode by −5 mV voltage steps relative to the holding potential of −65 mV. Asterisks indicate significant differences (p values indicated in Results).

Supported by the fact that SK-channel activators significantly increased the regularity of intrinsic Purkinje cell action potential firing, we further explored their possible therapeutic effects in alert *Cacna1a*^{S218L} mutant mice. Following topical application of 1-EBIO (cf. Material and Methods) the CV and CV2 values of ISSIs as well as the length of the climbing fiber pause decreased and the average simple spike firing frequency increased (all p values < 0.02), whereas the complex spike activity appeared unaffected in *Cacna1a*^{S218L} Purkinje cell activity (all p values > 0.5) (Fig. 10, *A*,*B*). 1-EBIO strongly reduced the occurrence of long ISSIs as indicated by the threefold reduction in the occurrence of ISSIs ≥ 100 ms ($4.5 \pm 0.7\%$ to $1.5 \pm 0.4\%$; $p < 0.002$) and also limited the occurrence of burst-pause firing: 1 of 21 recorded *Cacna1a*^{S218L} Purkinje cells showed burst-pause firing for 0.7% of the recording time. None of the WT Purkinje cells showed such burst-pause sequences: in fact, 1-EBIO also increased the regularity of WT simple spike firing pattern, as indicated by the decreased CV2-value in WT Purkinje cells ($p < 0.03$) (Fig. 10*A*). Thus, topically applied 1-EBIO promotes more regular simple spike firing in WT and, most effectively, in *Cacna1a*^{S218L} mutants.

In vivo application of SK-activator improved motor performance and Purkinje cell spiking patterns in *Cacna1a*^{S218L} mice

The positive effects of enhancing SK currents on Purkinje cell firing activity in *Cacna1a*^{S218L} mutants prompted us to test whether the motor behavior also improved by application of SK activators. To do so, we tested the effects of CHZ, which can be applied chronically by means of drinking water (Alviña and Khodakhah, 2010) (see Material and Methods), on the performance of WT and *Cacna1a*^{S218L} mutants on the accelerating rotarod. We first established a stable score for both WT (275 ± 6 s) and *Cacna1a*^{S218L} (111 ± 15 s) ($p < 0.001$) (Fig. 11*A*) and then supplied CHZ for the next 7 consecutive days. Whereas in WT CHZ did not affect the rotarod score, in *Cacna1a*^{S218L} mutants CHZ improved the performance in that their maximal rotation speed significantly increased (Fig. 11*A*,*B*) ($p = 0.02$). After we stopped the supply of CHZ the rotarod scores of the *Cacna1a*^{S218L} mutants returned to baseline values ($p = 0.03$ for CHZ scores relative to post-CHZ scores and $p = 0.8$ for post-CHZ scores relative to pre-CHZ scores), whereas in WT mice no change was observed ($p = 0.5$ for CHZ

scores relative to post-CHZ scores and $p = 0.7$ for post-CHZ scores relative to pre-CHZ scores).

To test whether the application of CHZ through the drinking water (Alviña and Khodakhah, 2010) indeed evoked a positive effect on Purkinje cell spiking patterns in *Cacna1a*^{S218L} mutants, we recorded the activity of 19 Purkinje cells after CHZ was applied for 6 consecutive days. We found that CHZ raised the average simple spike firing frequency significantly ($p < 0.001$) (Fig. 11*C*) and reduced the occurrence of ISSIs of ≥100 ms ($p < 0.004$). In addition, the pause in the simple spike firing following each complex spike was also significantly shorter than in untreated *Cacna1a*^{S218L} mutants ($p < 0.001$) (Fig. 11*D*). Moreover, during the burst-pause sequences, which occurred for 4.4 ± 2.5% of the recorded time in 6 of 19 recorded cells, the pauses were significantly shorter than in untreated *Cacna1a*^{S218L} mutants (76 ± 14 and 238 ± 75 s, respectively; $p < 0.03$). CHZ application did not result in a significant change in either the CV or CV2 values compared with untreated *Cacna1a*^{S218L} mutants, nor in altered complex spike firing patterns (all *p* values > 0.2) (Fig. 11*C*,*D*). Together these data show that CHZ not only alleviates the ataxic motor performance in *Cacna1a*^{S218L} mice, but also increases the simple spike firing frequency.

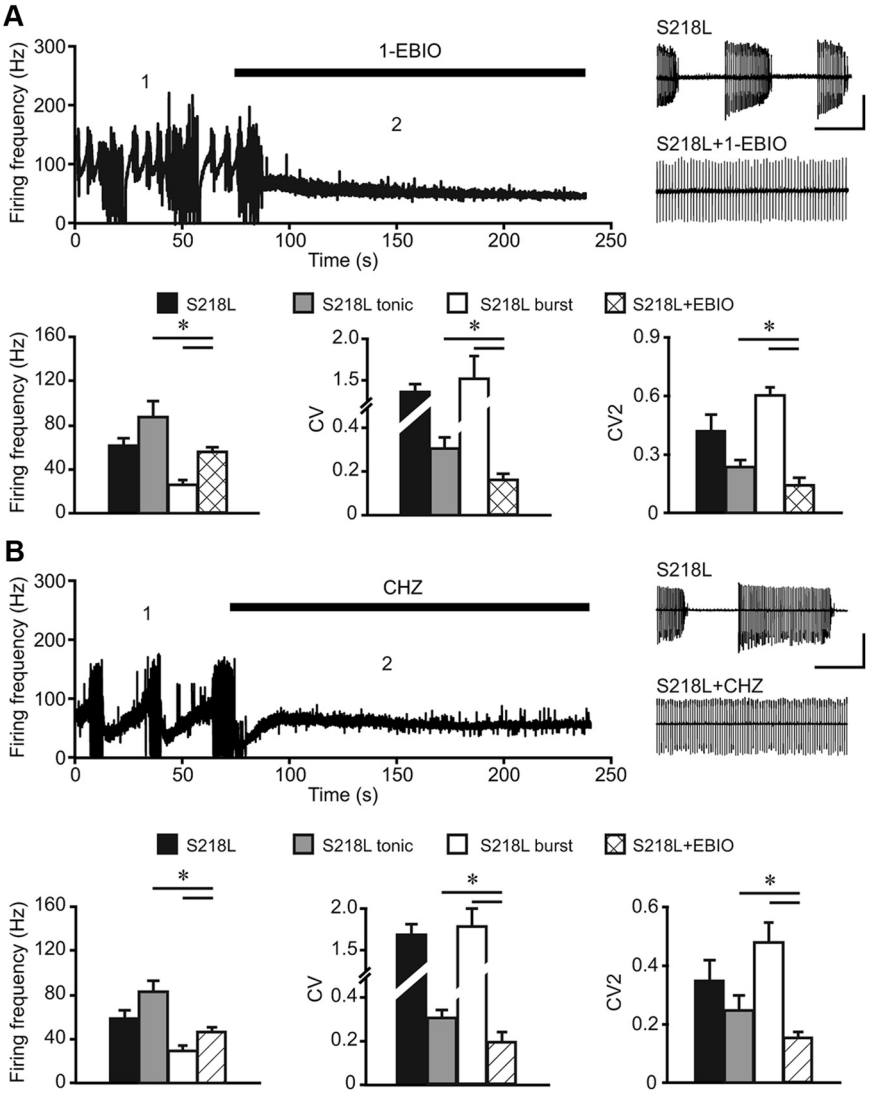

Figure 8. SK-channel activators 1-EBIO and CHZ reduce burst-like firing and thereby decrease irregular Purkinje cell firing in *Cacna1a*^{S218L} mutants. Firing frequency of intrinsic Purkinje cell activity in *Cacna1a*^{S218L} Purkinje cells while 1-EBIO (***A***) and CHZ (***B***) are washed into the recording bath. The numbers 1 and 2 indicate the time points at which the representative traces are shown, i.e., before and after application of 1-EBIO or CHZ in *Cacna1a*^{S218L} Purkinje cell (insets in ***A*** and ***B***). Scale bars: vertical, 100 pA; horizontal, 400 ms). Bar plots represent mean firing frequency, CV, and CV2 of intrinsic pacemaking activity of *Cacna1a*^{S218L} Purkinje cells as analyzed before and after the application of 1-EBIO (***A***; $n = 7$) or CHZ (***B***; $n = 8$). Note that only before the application of each of the drugs the *Cacna1a*^{S218L} Purkinje cells fired in tonic mode or burst-pause episodes and thus were analyzed accordingly. Asterisks indicate significant differences (*p* values indicated in Results).

Discussion

Previous studies have provided evidence that irregular Purkinje cell firing patterns contribute to cerebellar ataxia in *Cacna1a* mutants characterized by *decreased* $Ca_V2.1$-mediated Ca^{2+} influx (Hoebeek et al., 2005; Walter et al., 2006), but did not unravel why a *Cacna1a* mouse mutant with an *increased* $Ca_V2.1$-mediated Ca^{2+} influx is also ataxic. Here we reveal that the S218L mutation, which shifts the voltage dependence of $Ca_V2.1$-channel activation to more hyperpolarized values, renders Purkinje cells hyperexcitable and evokes irregular and slower Purkinje cell firing. Moreover, our study reveals that each of these effects of the *Cacna1a*^{S218L} mutation can be counteracted by increasing the SK-channel function: 1-EBIO and CHZ promote more regular simple spike firing by reducing the hyperexcitability of *Cacna1a*^{S218L} Purkinje cells and systemic CHZ application also improves the motor behavior of *Cacna1a*^{S218L} mutants.

Somatic and dendritic consequences of the S218L mutation in Purkinje cells

The S218L mutation in Purkinje cells causes a shift in the activation threshold of $Ca_V2.1$ channels to a more hyperpolarized level. This abnormal Ca^{2+} influx has specific effects on both Purkinje cell somata and dendrites. At the level of the soma, the negative shift in activation threshold of *Cacna1a*^{S218L} $Ca_V2.1$ channels (~−56 mV) results in a potential overlap with the initiation threshold of Na^+-dependent action potentials (Raman and Bean, 1997). At these membrane potentials, the resulting Ca^{2+} influx could serve as an additional depolarizing driving force (Fig. 3*D*) that affects the Na^+-channel activation threshold and its availability. In addition, Ca^{2+} influx via mutant $Ca_V2.1$ channels also elicits SK-channel activation (Fig. 6). Thus, it is likely that near the action potential initiation threshold $Ca_V2.1$-mediated currents in *Cacna1a*^{S218L} Purkinje cells not only coincide with Na^+ currents, but also evoke SK currents, a combination that is likely to affect Purkinje cell firing (Edgerton and Reinhart, 2003; Swensen and Bean, 2003; Womack and Khodakhah, 2004). Indeed, we found that during the bursting activity the action potential amplitude decreased and that long pauses consequently followed the bursts, which might be due to a decreased availability of Na^+ channels and an elevated level of SK currents, respectively. Thus, our data indicate that the

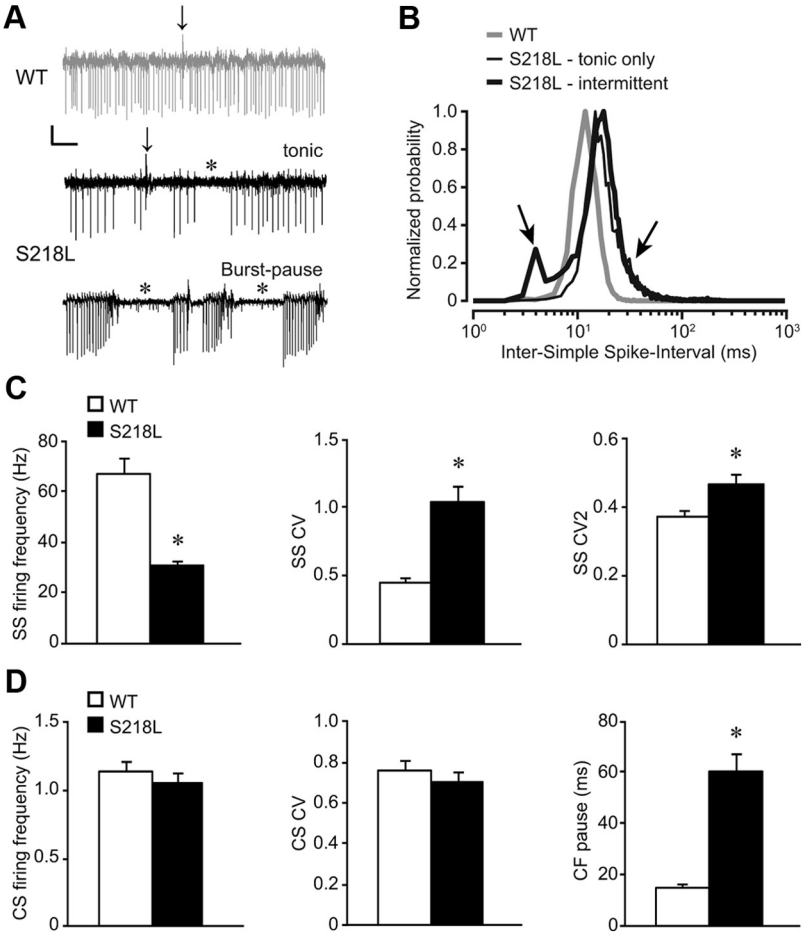

Figure 9. Irregular Purkinje cell firing in alert *Cacna1a*^{S218L} mutant mice. ***A***, Typical extracellular recordings of single unit Purkinje cell activity in an alert WT (top) and a *Cacna1a*^{S218L} (S218L; middle and bottom) mouse. Scale bars: vertical, 400 μV; horizontal, 100 ms. The middle example trace shows typical tonic Purkinje cell firing in *Cacna1a*^{S218L} mutants and the bottom trace shows typical burst-pause sequences in *Cacna1a*^{S218L} mutants. Arrows indicate complex spikes and all negative going events are simple spikes. Asterisks indicate long pauses without preceding complex spike activity. ***B***, Normalized probability distribution of all ISSIs from a typical example for a WT Purkinje cell (gray line), a tonically firing *Cacna1a*^{S218L} Purkinje cell (black line; tonic only), and a *Cacna1a*^{S218L} Purkinje cell that shows intermittent tonic and burst-pause firing (bold black line; intermittent). Note that the burst activity of simple spikes in *Cacna1a*^{S218L} is illustrated by the peak at short ISSIs (left arrow) and that both tonic and intermittently firing *Cacna1a*^{S218L} Purkinje cells show an increased occurrence of long pauses (right arrow). ***C***, Left, Average simple spike (SS) firing frequency. Middle, SS CV. Right, SS CV2 for WT (white; $n = 14$) and *Cacna1a*^{S218L} (black; $n = 25$). ***D***, Accompanying average complex spike (CS) firing frequency, CS CV, and length of climbing fiber (CF) pause. Asterisks indicate significant differences (p values indicated in Results).

S218L mutation affects the initiation threshold of action potentials and promotes somatic burst-firing.

In addition to these somatic effects, the S218L mutation affects dendritic membrane potentials. We found that *Cacna1a*^{S218L} Purkinje cells fire dendritic Ca^{2+} spikes in response to current injections that did not evoke dendritic Ca^{2+} spikes in WT Purkinje cells (Rancz and Häusser, 2006; Davie et al., 2008). More importantly, we found that *Cacna1a*^{S218L} Purkinje cells fire dendritic Ca^{2+} spikes in the absence of any current injection or synaptic input. These data suggest that the more negative activation threshold of $Ca_V2.1$ channels in *Cacna1a*^{S218L} Purkinje cells decreases the attenuation of somatic action potentials to such level that dendritic $Ca_V2.1$ channels can be activated and hence trigger dendritic Ca^{2+} spikes. In turn, the subsequent activation of dendritic SK channels during burst firing could also affect somatic action potential firing (Womack and Khodakhah, 2004). Thus, the combination of somatic and dendritic effects of the S218L mutation on Purkinje cell excitability appears to promote irregular activity patterns. Yet, we cannot rule out that our *in vitro* recording conditions may have, unlike those of other labs (Womack and Khodakhah, 2004; McKay and Turner, 2005), limited the occurrence of irregular Purkinje cell firing in WT (Häusser and Clark, 1997; Walter et al., 2006; Mark et al., 2011) and thus created a bias toward a larger effect of the S218L mutation.

Possible contributions of synaptic malfunction to cerebellar ataxia in *Cacna1a*^{S218L} mice

Our finding that burst-pause sequences in the simple spike activity of *Cacna1a*^{S218L} Purkinje cells occurred more frequently *in vitro* than *in vivo* raises the possibility that the S218L mutation not only affects Purkinje cell firing patterns through intrinsic mechanisms, but also by altering the activity and transmission of neurons upstream. In fact, all afferent neurons upstream of Purkinje cells including granule cells, molecular layer interneurons, and neurons in the inferior olive express $Ca_V2.1$ channels at their axon terminals (D'Angelo et al., 1997; Stephens et al., 2001; Kulik et al., 2004). The effects of the S218L mutation in granule cells were recently explored both at the somatic and axon terminal level. The negative shift of $Ca_V2.1$-mediated Ca^{2+} currents found in cerebellar granule cell somata (Tottene et al., 2005; van den Maagdenberg et al., 2010) align with our results in dissociated Purkinje cell somata (Fig. 1). In addition, at the granule cell axon terminal, the S218L mutation enhances the Ca^{2+} influx and decreases the paired-pulse facilitation of EPSCs due to the facilitated state of $Ca_V2.1$ channels (Adams et al., 2010). In principle, this could also lead to enhanced neurotransmitter release at this synapse in *Cacna1a*^{S218L} Purkinje cells and thereby enhance the hyperexcitability of Purkinje cells. Given that relatively small EPSPs robustly elicited burst-like firing in *Cacna1a*^{S218L} Purkinje cells, it is conceivable that the reported increase in granule cell output (Adams et al., 2010) directly affects Purkinje cell firing *in vivo*. In a similar fashion, the S218L mutation might also affect the neurotransmission at climbing fiber—Purkinje cell synapses, given the $Ca_V2.1$ dependence of both the neurotransmitter release and the postsynaptic response at this synapse (Schmolesky et al., 2002).

Apart from the excitatory input, the inhibitory inputs to Purkinje cells also might be subject to direct effects of the S218L mutation and thereby contribute to irregular Purkinje cell firing (Häusser and Clark, 1997; Mittmann and Häusser, 2007; Wulff et al., 2009). In cultured tissue derived from global *Cacna1a* knockout mice it was shown that the lack of $Ca_V2.1$-mediated Ca^{2+} influx reduces the inhibitory synaptic input to Purkinje cells (Lonchamp et al., 2009), which implicates that in *Cacna1a*^{S218L} the inhibitory transmission between molecular layer interneurons and Purkinje cells could be enhanced. Also the effects of the S218L mutation on $GABA_B$-mediated signaling could potentially

affect inhibitory inputs to Purkinje cells, as was previously shown in *Cacna1a*^{tottering} mutants (Zhou et al., 2003). Finally, the activity of *Cacna1a*^{S218L} molecular layer interneurons could also be affected by climbing fiber activity via spillover (Szapiro and Barbour, 2007). Future research should elucidate the effects of the S218L mutation on inhibitory transmission in the cerebellar cortex.

Effects of SK-channel activation on Purkinje cell activity and ataxia

How can SK-channel activators improve the spiking regularity of *Cacna1a*^{S218L} Purkinje cells? Since earlier studies showed that application of SK activators improve Purkinje cell spiking regularity and motor performance in mouse mutants with reduced $Ca_V2.1$-mediated Ca^{2+} influx (Walter et al., 2006; Alviña and Khodakhah, 2010), one would expect SK-channel blockers to alleviate irregular Purkinje cell firing in the *Cacna1a*^{S218L} Purkinje cells in which the $Ca_V2.1$-mediated Ca^{2+} influx is increased. Yet, our data showed that apamin enhances burst firing in *Cacna1a*^{S218L} Purkinje cells, which parallels the effects on WT Purkinje cell firing (Womack and Khodakhah, 2004). SK-channel activators, on the other hand, showed several positive effects on *Cacna1a*^{S218L} Purkinje cell firing patterns in our *in vitro* experiments. Application of 1-EBIO shifts the action potential threshold in *Cacna1a*^{S218L} Purkinje cells back to a near WT level (compare Figs. 3*D*, 7*C*) indicating that enhancing SK-channel activation counteracts the depolarizing effect of $Ca_V2.1$ channels. A similar mechanism could also explain the increased threshold of dendritic Ca^{2+} spikes following application of SK-channel activators. In addition, SK-channel activators turned out to enhance the AHP following each action potential *in vitro*, which increases regularity but decreases the action potential firing frequency (Womack and Khodakhah, 2004). Interestingly, *in vivo* application of 1-EBIO and CHZ both increased the action potential firing frequency (Table 2). This opposing effect of SK activators on the firing frequency of *Cacna1a*^{S218L} Purkinje cells recorded *in vitro* and *in vivo* may be explained by the effects of these drugs on cerebellar neurons upstream of Purkinje cells: in our *in vitro* recording conditions all synaptic inputs were blocked, whereas in our *in vivo* recordings all were intact. Apart from these network effects, the difference in type of applica-

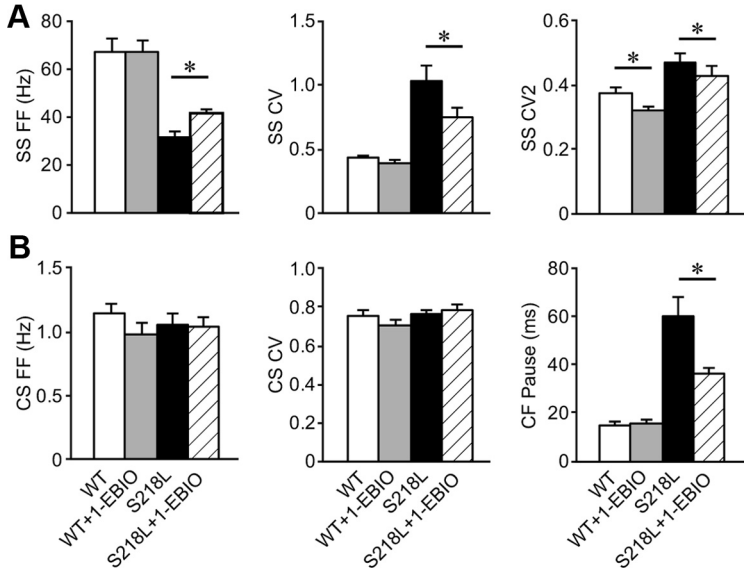

Figure 10. SK-channel activator 1-EBIO reduces irregularity and increases simple spike firing in alert *Cacna1a*^{S218L} mice. ***A***, Average simple spike (SS) firing frequency (FF) (left), SS CV (middle), and SS CV2 (right) for WT ($n = 14$), WT + 1-EBIO ($n = 13$), *Cacna1a*^{S218L} ($n = 25$), and *Cacna1a*^{S218L} + 1-EBIO ($n = 21$). ***B***, Accompanying average complex spike (CS) FF, CS CV, and climbing fiber (CF) pause. For comparison WT and *Cacna1a*^{S218L} Purkinje cell data are represented again (as in Fig. 9). Asterisks indicate significant differences (*p* values indicated in Results).

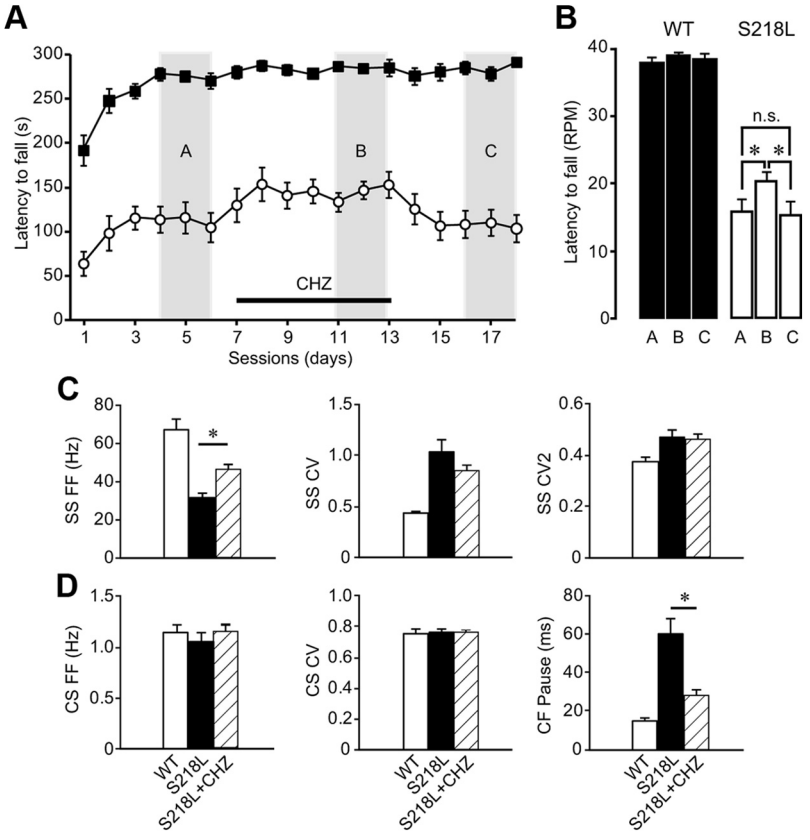

Figure 11. Oral administration of CHZ improves motor performance in *Cacna1a*^{S218L} mice and reduces long pauses in *Cacna1a*^{S218L} simple spike (SS) firing. ***A***, ***B***, The performance of *Cacna1a*^{S218L} mice ($n = 9$) and WT littermates ($n = 14$) were evaluated using an accelerating rotarod test on daily bases. CHZ was applied for 7 d (horizontal bar) after a stable score was achieved for 3 d. The performance was scored before, during, and after CHZ treatment by comparison of the latency to fall in time (***A***) and rotations per minute (***B***). Three days were averaged during each period as indicated by the vertical gray bars, ***A***, ***B***, and ***C***, respectively. ***C***, Average SS firing frequency (FF) (left), SS CV, and SS CV2 for WT ($n = 14$), *Cacna1a*^{S218L} ($n = 25$), and *Cacna1a*^{S218L} + CHZ ($n = 19$). ***D***, Accompanying average complex spike (CS) FF, CS CV, and climbing fiber (CF) pause. Asterisks indicate significant differences (*p* values indicated in Results).

Table 2. Effects of 1-EBIO and CHZ on Purkinje cell firing and motor behavior in Cacna1a^{S218L} mutant mice

	EBIO	CHZ
In vitro		
Firing frequency	↓	↓
CV	↓	↓
CV2	↓	↓
In vivo		
Firing frequency	↑	↑
CV	↓	=
CV2	↓	=
Climbing fiber pause	↓	↓
Motor behavior	Not tested	↑

In vitro: effects of 1-EBIO and CHZ on the tonic Purkinje cell action potential firing frequency, CV, and CV2 when applied separately to the recording chamber (Fig. 8). *In vivo*: effects of 1-EBIO and CHZ on the Purkinje cell simple spike firing pattern recorded in awake *Cacna1a*^{S218L} mutants when the drugs are applied to the surface of the brain following craniotomy (1-EBIO) (Fig. 10) or systemically (CHZ) (Fig. 11). The effects of systemically applied CHZ on the motor behavior were assessed using a rotarod test (Fig. 11). Note the similarity with the effects on motor behavior of chronic 1-EBIO application to *Cacna1a*^{tottering} mutant mice (Alviña and Khodakhah, 2010). Upward arrows indicate a significant increase, downward arrows a significant decrease, and equality marks indicate a nonsignificant effect; *p* values are reported in the corresponding results sections.

tion of SK activators *in vivo*, i.e., a topical (1-EBIO) and systemic (CHZ) approach, may also have had an impact on Purkinje cell firing, due to a difference in effect on other SK-expressing neurons (Stocker and Pedarzani, 2000). Moreover, the difference in type of application and effective concentration of both drugs in the different parts of the cerebellum may also account in part for the contrast between the effect of 1-EBIO and CHZ on the regularity of Purkinje cell firing (Table 2) (De Zeeuw et al., 2011). Yet, each of the conducted experiments revealed that SK activators are effective in reducing specific effects of the *Cacna1a*^{S218L} mutation on Purkinje cell firing.

Previous studies showed that systemic application of SK-channel activators may help patients and mutant mice characterized by reduced $Ca_V2.1$-mediated Ca^{2+} influx by promoting more regular Purkinje cell firing patterns (Alviña and Khodakhah, 2010). The current study suggests that SK activators should also improve motor performance of patients characterized by an increased $Ca_V2.1$-mediated Ca^{2+} influx, because of their impact on the action potential threshold and dendritic Ca^{2+}-spike activity. Together, these results advocate a general therapeutic approach, i.e., targeting Ca^{2+}-dependent K^+ channels may be beneficial for treating ataxia not only in patients suffering from a decreased Ca^{2+} influx, but also in those suffering from an increased Ca^{2+} influx in their Purkinje cells.

References

Adams PJ, Rungta RL, Garcia E, van den Maagdenberg AM, MacVicar BA, Snutch TP (2010) Contribution of calcium-dependent facilitation to synaptic plasticity revealed by migraine mutations in the P/Q-type calcium channel. Proc Natl Acad Sci U S A 107:18694–18699.

Alviña K, Khodakhah K (2010) KCa channels as therapeutic targets in episodic ataxia type-2. J Neurosci 30:7249–7257.

Catterall WA, Dib-Hajj S, Meisler MH, Pietrobon D (2008) Inherited neuronal ion channelopathies: new windows on complex neurological diseases. J Neurosci 28:11768–11777.

Cingolani LA, Gymnopoulos M, Boccaccio A, Stocker M, Pedarzani P (2002) Developmental regulation of small-conductance Ca2+-activated K+ channel expression and function in rat Purkinje neurons. J Neurosci 22: 4456–4467.

D'Angelo E, De Filippi G, Rossi P, Taglietti V (1997) Synaptic activation of Ca2− action potentials in immature rat cerebellar granule cells in situ. J Neurophysiol 78:1631–1642.

Davie JT, Clark BA, Häusser M (2008) The origin of the complex spike in cerebellar Purkinje cells. J Neurosci 28:7599–7609.

Devor DC, Singh AK, Frizzell RA, Bridges RJ (1996) Modulation of Cl^- secretion by benzimidazolones. I. Direct activation of a Ca^{2+}-dependent K^+ channel. Am J Physiol 271:L775–784.

De Zeeuw CI, Hoebeek FE, Bosman LW, Schonewille M, Witter L, Koekkoek SK (2011) Spatiotemporal firing patterns in the cerebellum. Nat Rev Neurosci 12:327–344.

Edgerton JR, Reinhart PH (2003) Distinct contributions of small and large conductance Ca2+-activated K+ channels to rat Purkinje neuron function. J Physiol 548:53–69.

Eggermont JJ (1990) The correlative brain (Braitenberg, V, ed). New York: Springer.

Fletcher CF, Lutz CM, O'Sullivan TN, Shaughnessy JD Jr, Hawkes R, Frankel WN, Copeland NG, Jenkins NA (1996) Absence epilepsy in tottering mutant mice is associated with calcium channel defects. Cell 87:607–617.

Häusser M, Clark BA (1997) Tonic synaptic inhibition modulates neuronal output pattern and spatiotemporal synaptic integration. Neuron 19:665–678.

Hoebeek FE, Stahl JS, van Alphen AM, Schonewille M, Luo C, Rutteman M, van den Maagdenberg AM, Molenaar PC, Goossens HH, Frens MA, De Zeeuw CI (2005) Increased noise level of purkinje cell activities minimizes impact of their modulation during sensorimotor control. Neuron 45:953–965.

Hoebeek FE, Witter L, Ruigrok TJ, De Zeeuw CI (2010) Differential olivocerebellar cortical control of rebound activity in the cerebellar nuclei. Proc Natl Acad Sci U S A 107:8410–8415.

Holt GR, Softky WR, Koch C, Douglas RJ (1996) Comparison of discharge variability in vitro and in vivo in cat visual cortex neurons. J Neurophysiol 75:1806–1814.

Hounsgaard J, Yamamoto C (1979) Dendritic spikes in Purkinje cells of the guinea pig cerebellum studied in vitro. Exp Brain Res 37:387–398.

Jörntell H, Ekerot CF (2006) Properties of somatosensory synaptic integration in cerebellar granule cells *in vivo*. J Neurosci 26:11786–11797.

Jouvenceau A, Eunson LH, Spauschus A, Ramesh V, Zuberi SM, Kullmann DM, Hanna MG (2001) Human epilepsy associated with dysfunction of the brain P/Q-type calcium channel. Lancet 358:801–807.

Kitamura K, Häusser M (2011) Dendritic calcium signaling triggered by spontaneous and sensory-evoked climbing fiber input to cerebellar Purkinje cells *in vivo*. J Neurosci 31:10847–10858.

Kors EE, Terwindt GM, Vermeulen FL, Fitzsimons RB, Jardine PE, Heywood P, Love S, van den Maagdenberg AM, Haan J, Frants RR, Ferrari MD (2001) Delayed cerebral edema and fatal coma after minor head trauma: role of the CACNA1A calcium channel subunit gene and relationship with familial hemiplegic migraine. Ann Neurol 49:753–760.

Kulik A, Nakadate K, Hagiwara A, Fukazawa Y, Luján R, Saito H, Suzuki N, Futatsugi A, Mikoshiba K, Frotscher M, Shigemoto R (2004) Immunocytochemical localization of the alpha 1A subunit of the P/Q-type calcium channel in the rat cerebellum. Eur J Neurosci 19:2169–2178.

Llinás R, Sugimori M (1980a) Electrophysiological properties of in vitro Purkinje cell somata in mammalian cerebellar slices. J Physiol 305:171–195.

Llinás R, Sugimori M (1980b) Electrophysiological properties of in vitro Purkinje cell dendrites in mammalian cerebellar slices. J Physiol 305:197–213.

Lonchamp E, Dupont JL, Doussau F, Shin HS, Poulain B, Bossu JL (2009) Deletion of Cav2.1(alpha1(A)) subunit of Ca2+-channels impairs synaptic GABA and glutamate release in the mouse cerebellar cortex in cultured slices. Eur J Neurosci 30:2293–2307.

Mark MD, Maejima T, Kuckelsberg D, Yoo JW, Hyde RA, Shah V, Gutierrez D, Moreno RL, Kruse W, Noebels JL, Herlitze S (2011) Delayed postnatal loss of P/Q-type calcium channels recapitulates the absence epilepsy, dyskinesia, and ataxia phenotypes of genomic *Cacna1a* mutations. J Neurosci 31:4311–4326.

McKay BE, Turner RW (2005) Physiological and morphological development of the rat cerebellar Purkinje cell. J Physiol 567:829–850.

Mintz IM, Venema VJ, Swiderek KM, Lee TD, Bean BP, Adams ME (1992) P-type calcium channels blocked by the spider toxin omega-Aga-IVA. Nature 355:827–829.

Mittmann W, Häusser M (2007) Linking synaptic plasticity and spike output at excitatory and inhibitory synapses onto cerebellar Purkinje cells. J Neurosci 27:5559–5570.

Mori Y, Wakamori M, Oda S, Fletcher CF, Sekiguchi N, Mori E, Copeland NG, Jenkins NA, Matsushita K, Matsuyama Z, Imoto K (2000) Reduced voltage sensitivity of activation of P/Q-type Ca2+ channels is associated

with the ataxic mouse mutation rolling Nagoya (tg(rol)). J Neurosci 20:5654–5662.

Ophoff RA, Terwindt GM, Vergouwe MN, van Eijk R, Oefner PJ, Hoffman SM, Lamerdin JE, Mohrenweiser HW, Bulman DE, Ferrari M, Haan J, Lindhout D, van Ommen GJ, Hofker MH, Ferrari MD, Frants RR (1996) Familial hemiplegic migraine and episodic ataxia type-2 are caused by mutations in the Ca2+ channel gene CACNL1A4. Cell 87:543–552.

Pedarzani P, Mosbacher J, Rivard A, Cingolani LA, Oliver D, Stocker M, Adelman JP, Fakler B (2001) Control of electrical activity in central neurons by modulating the gating of small conductance Ca2+-activated K+ channels. J Biol Chem 276:9762–9769.

Pietrobon D (2007) Familial hemiplegic migraine. Neurotherapeutics 4:274–284.

Pietrobon D (2010) CaV2.1 channelopathies. Pflugers Arch 460:375–393.

Raman IM, Bean BP (1997) Resurgent sodium current and action potential formation in dissociated cerebellar Purkinje neurons. J Neurosci 17:4517–4526.

Raman IM, Bean BP (1999) Ionic currents underlying spontaneous action potentials in isolated cerebellar Purkinje neurons. J Neurosci 19:1663–1674.

Rancz EA, Häusser M (2006) Dendritic calcium spikes are tunable triggers of cannabinoid release and short-term synaptic plasticity in cerebellar Purkinje neurons. J Neurosci 26:5428–5437.

Schmolesky MT, Weber JT, De Zeeuw CI, Hansel C (2002) The making of a complex spike: ionic composition and plasticity. Ann N Y Acad Sci 978:359–390.

Stephens GJ, Morris NP, Fyffe RE, Robertson B (2001) The Cav2.1/alpha1A (P/Q-type) voltage-dependent calcium channel mediates inhibitory neurotransmission onto mouse cerebellar Purkinje cells. Eur J Neurosci 13:1902–1912.

Stocker M, Pedarzani P (2000) Differential distribution of three Ca2+-activated K+ channel subunits, SK1, SK2, and SK3, in the adult rat central nervous system. Mol Cell Neurosci 15:476–493.

Stuart G, Häusser M (1994) Initiation and spread of sodium action potentials in cerebellar Purkinje cells. Neuron 13:703–712.

Swensen AM, Bean BP (2003) Ionic mechanisms of burst firing in dissociated Purkinje neurons. J Neurosci 23:9650–9663.

Szapiro G, Barbour B (2007) Multiple climbing fibers signal to molecular layer interneurons exclusively via glutamate spillover. Nat Neurosci 10:735–742.

Tottene A, Pivotto F, Fellin T, Cesetti T, van den Maagdenberg AM, Pietrobon D (2005) Specific kinetic alterations of human CaV2.1 calcium channels produced by mutation S218L causing familial hemiplegic migraine and delayed cerebral edema and coma after minor head trauma. J Biol Chem 280:17678–17686.

van den Maagdenberg AM, Haan J, Terwindt GM, Ferrari MD (2007) Migraine: gene mutations and functional consequences. Curr Opin Neurol 20:299–305.

van den Maagdenberg AM, Pizzorusso T, Kaja S, Terpolilli N, Shapovalova M, Hoebeek FE, Barrett CF, Gherardini L, van de Ven RC, Todorov B, Broos LA, Tottene A, Gao Z, Fodor M, De Zeeuw CI, Frants RR, Plesnila N, Plomp JJ, Pietrobon D, Ferrari MD (2010) High cortical spreading depression susceptibility and migraine-associated symptoms in Ca(v)2.1 S218L mice. Ann Neurol 67:85–98.

Walter JT, Alviña K, Womack MD, Chevez C, Khodakhah K (2006) Decreases in the precision of Purkinje cell pacemaking cause cerebellar dysfunction and ataxia. Nat Neurosci 9:389–397.

Womack MD, Khodakhah K (2004) Dendritic control of spontaneous bursting in cerebellar Purkinje cells. J Neurosci 24:3511–3521.

Wulff P, Schonewille M, Renzi M, Viltono L, Sassoè-Pognetto M, Badura A, Gao Z, Hoebeek FE, van Dorp S, Wisden W, Farrant M, De Zeeuw CI (2009) Synaptic inhibition of Purkinje cells mediates consolidation of vestibulo-cerebellar motor learning. Nat Neurosci 12:1042–1049.

Wylie DR, De Zeeuw CI, Simpson JI (1995) Temporal relations of the complex spike activity of Purkinje cell pairs in the vestibulocerebellum of rabbits. J Neurosci 15:2875–2887.

Zhou YD, Turner TJ, Dunlap K (2003) Enhanced G protein-dependent modulation of excitatory synaptic transmission in the cerebellum of the Ca2+ channel-mutant mouse, tottering. J Physiol 547:497–507.